Cloud Process Coupling and Time Integration in the E3SM Atmosphere Model

Sean Patrick Santos[1], Peter M. Caldwell[2], and Christopher S. Bretherton[1,3]

[1]Center for Climate Systems Research, Columbia University, and NASA Goddard Institute for Space Studies, New York, NY, USA
[2]Lawrence Livermore National Laboratory, Livermore, CA, USA
[3]Department of Atmospheric Sciences, University of Washington, Seattle, WA, USA

Key Points:

- Changing time step has as large an effect on E3SMv1's climate as doubling horizontal resolution.
- Shorter timesteps dry the atmosphere and increase surface precipitation.
- Coupling between processes is the most important source of model time step sensitivity.

Corresponding author: Sean Patrick Santos, spsantos@uw.edu

Abstract

In this study, we find significant sensitivity to the choice of time step for the Energy Exascale Earth System Model's atmospheric component, leading to large decreases in the magnitude of cloud forcing when the time step is reduced to 10 seconds. Reducing the time step size for the microphysics increases precipitation, leading to a drying of the atmosphere and an increase in surface evaporation. This effect is amplified when the microphysics is substepped together with other cloud physics processes. Coupling the model's dynamics and physics more frequently reduces cloud fraction at lower altitudes, while producing more cloud liquid at higher altitudes. Reducing the deep convection time step also reduces low cloud mass and cloud fraction. Together, these results suggest that cloud physics in a global circulation model can depend strongly on time step, and in particular on the frequency with which cloud-related processes are coupled with each other and with the model dynamics.

Plain Language Summary

Computer simulations of the Earth's atmosphere take the state of the atmosphere at one point in time, then predict the state of the atmosphere a short interval of time into the future. The length of this time interval is known as the "time step". By doing this repeatedly, models can produce a simulated history of the atmosphere for years or even centuries. A smaller time step size requires more computer time, but should ideally lead to more accurate results. In this study we reduce the time step for the atmosphere in the Energy Exascale Earth System Model from half an hour to ten seconds. The simulation with a smaller time step has more rain, which removes water from the atmosphere and reduces the fraction of the Earth's surface that is covered by clouds. We also experiment with changing the time step for only some parts of the model and not others. We find that the effects of the time step size on the model are related mostly to the frequency of coupling between processes rather than the time step used for any individual processes.

1 Introduction

1.1 Time Step Sensitivity in AGCMs

Time integration strategies for atmospheric general circulation models (AGCMs) have grown more complex, both due to an increase in the number of separate processes within a model (allowing individual parameterizations to adopt different time integration strategies from the "host" model), and due to changes in process coupling. The latter include modifications that allow different processes to be run concurrently (Balaji et al., 2016; Donahue & Caldwell, 2020), as well as process coupling methods that apply the effects of faster processes separately from the effects of slower processes (Beljaars et al., 2004, 2018; Dubal et al., 2005; Diamantakis et al., 2007; Walters et al., 2019). This increase in complexity means that there is often no single time step for the model, but rather a set of interrelated time steps controlling the rate at which various calculations are performed and allowed to interact. This increased complexity can be daunting, but it also provides the opportunity to conduct more detailed experiments regarding the effect of temporal resolution on AGCMs. Past research has established that certain cloud processes can be disproportionately responsible for time integration error in AGCMs (Wan et al., 2015). When the time steps used for particular processes can easily be adjusted independently from one another, it becomes possible to study the time step sensitivity of these processes with minimal changes to the model code.

This approach has already been used frequently in microphysics parameterization development. Posselt and Lohmann (2008) added substepping of rain production and sedimentation to ECHAM5 to better represent prognostic precipitation. Chosson et al.

(2014) used substepping to test the time step sensitivity of the Milbrandt and Yau two-moment scheme in the Canadian Global Environmental Multiscale (GEM) model. Gettelman et al. (2015) examined the time step sensitivities of version 2 of the Morrison-Gettelman scheme (MG2) in combination with different cloud macrophysics schemes in the Community Atmosphere Model (CAM). The time step sensitivity of microphysics schemes has also been tested in 1D kinematic drivers (Chosson et al., 2014; Gettelman & Morrison, 2015) and other 0D and 1D frameworks (Riette, 2020; Santos et al., 2020).

Regarding AGCMs as a whole, a number of studies have found that these models are sensitive to choice of model time step and integration strategy. Wan et al. (2013) discusses the effect of changes to the time stepping scheme on sulfuric acid gas concentrations in ECHAM-HAM, and Gross et al. (2018) mentions that one version of the ECHAM5 atmosphere model exhibits a much larger response to a doubling of CO_2 at a 40 minute time step than at a 5 minute time step. The merits of different dynamics-physics coupling strategies has also been examined for a number of models, including the ECMWF's Integrated Forecasting System (IFS) (Beljaars et al., 2004) and the Met Office Unified Model (Diamantakis et al., 2007; Walters et al., 2019). Beljaars et al. (2004) also notes some specific effects of reducing the time step of IFS, including decreasing the mean 10 meter wind speed, reducing the frequency of heavy precipitation events, and increasing the cloud base mass fluxes in the convection schemes. However, these kinds of experiments, which explore the time step sensitivity of a given AGCM by comparing simulations using the same model with different time steps, are relatively rare (Gross et al., 2018). To the best of our knowledge, most published experiments of this type have been performed on the CAM family of atmosphere models, which we will focus on for the remainder of this section.

Prior research using the Community Atmosphere Model, versions 3 and 4, (CAM3/4), as well as its predecessor, the Community Climate Model, version 3, suggests that time step size for a AGCM has significant effects on precipitation in an aquaplanet simulation, particularly in the intertropical convergence zone (ITCZ) (Williamson & Olson, 2003; Williamson, 2008; Mishra et al., 2008). Decreasing the time step increases total precipitation in the ITCZ and the frequency of extreme precipitation events. The partition of precipitation between the large-scale and convective parameterizations is also affected, with an increase in the large-scale precipitation being responsible for the aforementioned effects. For CAM3, the increase in total precipitation was found to be dependent on an increase in evaporation at the surface, which in turn was due to an increase in wind speed and a decrease in specific humidity near the surface (Mishra et al., 2008). Further research using CAM3 for real-planet simulations confirmed these results, and showed that the increased evaporation, in addition to producing increased precipitable water (and precipitation), also produced a larger cloud fraction at low altitude and an increased magnitude of radiative cloud forcing (Mishra & Shanay, 2011). Williamson (2013), using CAM4, found that the time step of the convective schemes, and in particular their rate of coupling with other processes, controlled the repartitioning of precipitation between large-scale and convective processes. Wan et al. (2014) also found increases in cloud fraction and ice and liquid water path in CAM5, at least in December-January-February averages, as well as increased large-scale precipitation.

Yu and Pritchard (2015) experimented with changes in the global model time step for a superparameterized version of CAM3 (SPCAM3), without changing its cloud resolving model's time step. Decreasing the CAM time step increased overall precipitation in SPCAM3, as well as the frequency of heavy precipitation events, which also happened for CAM3. However, reducing the time step size in SPCAM3 *decreased* precipitable water, decreased both liquid and ice water path, and ultimately decreased the magnitude of radiative cloud forcings. This was hypothesized to be due to changes in convective organization, producing an increase in precipitation efficiency and effectively drying out the atmosphere.

Although both CAM3 and SPCAM3 experience similar increases in surface evaporation and precipitation (which must match in the long run, to balance the water budget), the proposed mechanisms driving these changes are different. In effect, the increased evaporation in CAM3 "pushes" more precipitable water into the atmosphere, eventually forcing an increase in condensation and precipitation to remove this water, while the increased precipitation efficiency in SPCAM3 "pulls" water out of the atmosphere, drying it out and encouraging evaporation to replace the lost water.

This paper analyzes time step sensitivity in the Energy Earth System Model, version 1 (E3SMv1), and specifically its atmospheric component, the E3SM Atmosphere Model, version 1 (EAMv1). EAMv1 shares very little of its physics with CAM3, and almost none with SPCAM3. Nevertheless, EAMv1 is descended from CAM3 and uses the same general strategies for coupling the physics parameterizations, dynamics, and surface components. We have recently examined the effect of time step size on a specific parameterization used in EAMv1, the Morrison-Gettelman microphysics version 2 (MG2). We found that the total precipitation was not sensitive to changes to the MG2 time step alone, though we did see a mild increase in the ratio of stratiform to convective precipitation (Santos et al., 2020). While the details of the precipitation physics and the vertical distribution of rain mass changed significantly at small time steps, the effect on total precipitation reaching the surface was mild.

1.2 Time Integration Error in a Simple Model

In order to lay the groundwork for later discussions of time step sensitivity in E3SMv1, we should briefly discuss the difference between the error that arises from using a finite time step to integrate a particular physical process, and the error that arises from infrequent coupling between processes. To illustrate the difference, let us consider the same simple saturation model described by Williamson (2013). The model can be described succinctly as

$$\frac{dq}{dt} = \alpha - \frac{\max(q - q_s, 0)}{\tau} \tag{1}$$

where q is specific humidity that changes over time t, q_s is the saturation specific humidity, α is a constant source of humidity from a process labeled "D", τ is a relaxation timescale governing the removal of supersaturation by a process labeled "P". For an initially saturated or supersaturated state q_0, this model has the exact solution

$$q = q_{eq} + (q_0 - q_{eq})e^{-t/\tau} \tag{2}$$

where $q_{eq} = q_s + \alpha\tau$ is the equilibrium specific humidity that the model approaches asymptotically.

Figure 1a shows different solution methods for this model for a saturated initial condition. The exact solution exponentially approaches a highly saturated state. Williamson discusses the impact of solving this equation using a sequentially split method with a finite coupling time step (which we will call Δt_{cpl}). At each time step, process D adds $\alpha\Delta t_{cpl}$ to the specific humidity, which is then removed by process P at an exponentially decaying rate. If q^n denotes the specific humidity at the end of the n-th time step, then this scheme can be summed up by

$$q^{n+1} - q_s = (q^n - q_s + \alpha\Delta t_{cpl})e^{-\Delta t_{cpl}/\tau} \tag{3}$$

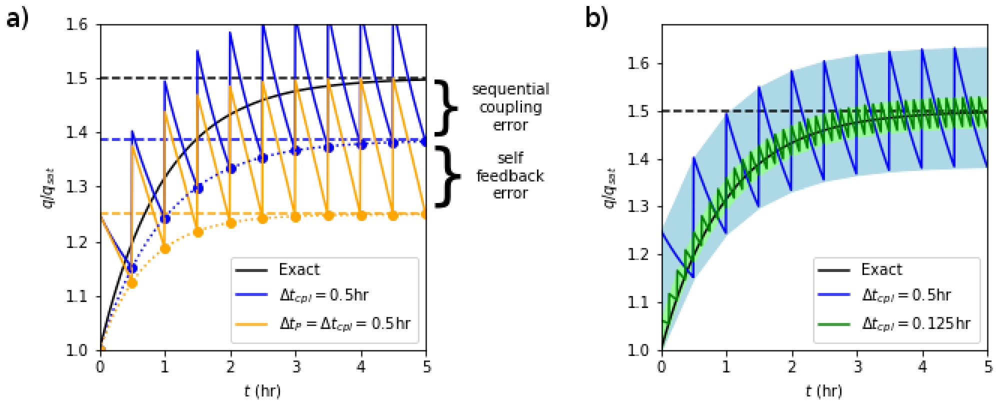

Figure 1. Solutions to the simple model used in Williamson (2013), with $\alpha = 0.5$ and $\tau = 1$, starting at $q = q_{sat}$. a) The exact solution for this model (black line) approaches a supersaturated equilibrium state (black dashes). Injecting water vapor using a finite coupling interval produces less saturated end-of-time-step values (blue dots), and causes the humidity to vary wildly depending on when it is measured within each time step (blue line). The end-of-time-step values approach a equilibrium with less supersaturation (blue dashes). Using the forward Euler method with the same coarse time step produces even less saturated outputs (orange dots, orange line), reaching a less supersaturated equilibrium (orange dashes). b) Black and blue trajectories as before, with blue shading covering the range of possible trajectories that could be obtained by recording the output at different points in the time step. Using a time step that is only 1/4 as large reduces the range of possible outputs proportionally (green line and shading).

which is equation (8) from Williamson (2013).

This sequentially split scheme demonstrates the effect of coupling error in this toy model, but it assumes that process P is integrated exactly (hence the exponential multiplicand). We can instead integrate P using the forward Euler method, using M substeps for each model coupling time step, i.e. the substeps are of size $\Delta t_P = \Delta t_{cpl}/M$. Using $q^{n,m}$ to denote the state after the m-th substep in the n-th coupling time step, this method can be summed up as

$$\begin{aligned} q^{n,0} &= q^n + \alpha \Delta t_{cpl} \\ q^{n,m} &= q^{n,m-1} - (q^{n,m-1} - q_s)\Delta t_P/\tau \\ q^{n+1} &= q^{n,M} \end{aligned} \tag{4}$$

If we say that $M = 1$, i.e. that P runs at the model time step with no substepping, then $\Delta t_P = \Delta t_{cpl}$, and our scheme simplifies to

$$q^{n+1} - q_s = [q^n - q_s + \alpha\Delta t_{cpl}]\,[1 - \Delta t_{cpl}/\tau] \tag{5}$$

This scheme has the lowest equilibrium specific humidity of all.

We can interpret these results as demonstrating the effects of two different forms of time discretization error on the model results. The exact solution to (1) shows that process P is ineffective at removing supersaturation when water vapor is introduced at a steady rate by process D. Using a sequential split method with a large coupling time step causes the effect of D to be introduced to P as a series of large shocks, causing P to overreact to these large increases in saturation. Additionally, we can see that if the effect of P is solved using the forward Euler method at a coarse time step, P does not experience the negative feedback that would result from its own removal of water vapor during a single time step. These two sources of numerical error are comparable in size, and both act to strengthen the effect of process P.

An AGCM such as EAMv1 obviously cannot be analyzed as easily as as this single-variable linear differential equation. Nonetheless, time integration error for any given process in the model can still be attributed to two distinct sources. First, we have the "coupling error", resulting from each process responding to all other processes at the finite coupling time step. Since EAMv1 uses sequential updates to couple its physics suite, a coarse coupling time step introduces a form of spurious temporal variability, as each process "sees" the effect of all other parameterizations as a sudden shock that occurs every coupling time step. Second, we have a "self-feedback error", resulting from each process responding to its own effect on the atmospheric state at finite intervals. Each process is solved using its own time integration method (most commonly the forward Euler method), resulting in an error that depends on both the process's time step and the particular integration method used.

Figure 1b further shows that, for a model using a simple first-order sequential splitting method, the coupling error is dominated by the effect of process ordering. While the output state after process P is less saturated than the exact solution, the state after process D is more saturated, so the sign of the error depends on when the output is recorded. If the time step is reduced, the output state after P and the output state after D both approach the exact solution, and the effect of process ordering becomes less important. There are also sequential splitting methods that use a symmetric combination of different process orderings to produce results, such as Strang splitting or symmetrically-weighted sequential splitting, and these can produce second-order accuracy (Strang, 1968).

Reducing all time steps present in a model allows us to measure the time step sensitivity of that model, but it does not directly tell us whether the effect of changing the time step is attributable to any particular process, nor whether the time step sensitivity is related to coupling error or self-feedback error. By varying coupling step sizes independently from the substeps for particular parameterizations, we are better situated to attribute time step sensitivity to particular parameterizations, and to determine the particular physical mechanisms by which changes to the model numerics can result in a different climate.

2 Model Description and Simulation Strategy

2.1 The E3SM Atmosphere Model

E3SMv1 is an earth system model developed by the U.S. Department of Energy, focusing on three main research topics: (1) the water cycle, (2) the cryosphere, and (3) biogeochemistry (Golaz et al., 2019). Its atmospheric component, EAMv1, is run at a standard resolution of $\sim$100 km (1°) (Rasch et al., 2019; Xie et al., 2018). At this resolution, the physics parameterizations, dynamical core, and surface components are coupled at a time step of 30 minutes (1800 seconds), with the various processes and dynamical core typically coupled using a "sequential split" method. This means that for each time step, each parameterization accepts a state that has already been updated by applying the effects of previous parameterizations, and so at large time steps, the model physics depends on the order in which these updates are applied (Donahue & Caldwell, 2018). (This should be irrelevant for sufficiently small time steps, assuming that the model

Scheme Name	Processes Represented	Default Time Step Size(s)
Zhang-McFarlane scheme (ZM)	Deep Convection	1800s
Cloud Layers Unified By Binormals (CLUBB)	Turbulence Shallow Convection Stratiform Clouds	300s (looped with MG2)
Morrison-Gettelman scheme version 2 (MG2)	Stratiform Microphysics	300s (looped with CLUBB)
Four-mode Modal Aerosol Module (MAM4)	Aerosol-related processes	1800s (different processes evaluated at different points in the time step)
Rapid Radiative Transfer Model for GCMs (RRTMG)	Radiative transfer	Rates applied: 1800s Rates recalculated: 3600s
Surface coupling	Surface fluxes	1800s
Linearized ozone chemistry (LINOZ2)	Ozone chemistry	1800s
Gravity wave scheme	Gravity wave propagation and breaking	1800s
Spectral element dynamics (HOMME)	Dynamics Tracer Advection	Vertical remapping: 900s Dynamics/Advection: 300s Hyperviscosity subcycle: 100s

Table 1. EAMv1 parameterizations and corresponding time steps for a Δx $\approx$100 km run using default settings

converges in this limit to the true solution of its spatially discretized motivating equations.)

Table 1 shows a summary of the main parameterizations of EAMv1 in the order that they run in an atmospheric time step, as well as the default time steps for these schemes at standard resolution. Variables that are only calculated once per time step (e.g. surface fluxes) are typically recorded at whatever point in the time step they are calculated. However, state variables and diagnostics that are affected by many parameterizations are recorded at the point in the time step just before the radiation model runs. (This includes temperature, humidity, and cloud-related properties such as liquid water content and cloud fraction.) The outputs for EAMv1 thus reflect the model state after the effects of stratiform cloud and aerosol microphysics have been applied, but before the effects of radiative transfer are applied.

The summary in Table 1 is by necessity a broad overview, since each of these parameterizations is a complex piece of software in its own right. In general, we can say that (a) the dynamics-physics coupling time step is the maximum allowed time step for any physics parameterization, and (b) most physics parameterizations couple to one another at the same frequency as they couple to the dynamics. However, there are two exceptions to these rules. Tendencies due to radiative transfer are only recalculated every hour by default, i.e. every other coupling time step. The CLUBB and MG2 parameterizations, on the other hand, are coupled using a shorter time step, since they are substepped within a single loop. Each "sees" the updates from the other during each of their smaller 300 second time steps.

The climate of EAMv1 using default settings is extensively documented, for instance in Golaz et al. (2019), Rasch et al. (2019), and Xie et al. (2018). This work will focus on the climatological differences between various modified runs using shorter time steps and a control EAMv1 run at default settings.

This approach allows us to broadly discuss the magnitude and nature of time integration error in EAMv1. We note that the model was developed and tuned for much longer time steps than we use here, and the tuning parameters are likely set so as to partially cancel this time integration error. While the ALL10 run described below should have a dramatically lower *time integration* error, we do not assert that it is "better" than the default configuration as a production model, and in fact it would require significant retuning to be usable at all.

2.2 Simulation Details

We ran E3SMv1 at a $\sim$100 km atmospheric resolution (ne30_ne30 grid) with standard E3SMv1 tuning and prescribed sea surface temperature. These runs were performed using a maintenance version of E3SM 1.1 (the version corresponding to the git hash 25c94366) with pre-industrial forcings (E3SMv1 compset F1850C5AV1C-04P2) unless otherwise specified, and all had prescribed sea surface temperature (SST) and sea ice extent.

The control run (CTRL) is an out-of-the-box run using default settings. We compare this to a new run (ALL10) that changed the atmosphere's dynamics-physics-surface coupling time step, known as "dtime" in the model settings, to 10 s. This time step is chosen to be as small as we could reasonably afford, within the constraints of the computing power we had available for this study. CTRL and ALL10 simulations are both 3 years in length. Results based on years 1-2 were unchanged after adding year 3, which gives us confidence that 3 years is long enough to draw robust conclusions.

Users typically consider the dtime setting to equivalent to the atmosphere model time step, but there are three ways in which this is not quite true. First, as noted earlier, the radiative transfer rates are updated only once per hour, regardless of dtime. While the ALL10 run does not change this update frequency, our tests with shorter runs show that the model is not especially sensitive to this time step. Second, the dynamics and cloud physics contain some substepping by default, though none run at a time step as small as 10 s. In the ALL10 run, we disable these forms of substepping, so that all major dynamics and physics processes run at the same small time step. Third, because the dtime setting also governs the rate at which EAMv1 exchanges information with the surface components, changing it forces a change in the land and sea ice components, which must run at a 10 s time step as well.

To investigate which processes within EAMv1 were most responsible for its overall time step sensitivity, we configured a series of runs using built-in options to substep individual parameterizations at a 10 s time step. These runs include DYN10, which substepped EAMv1's spectral element dynamical core, CLUBB10, which substepped the CLUBB cloud physics parameterization, and MICRO10, which substepped the MG2 stratiform microphysics. Typically CLUBB and MG2 are substepped together within a single loop, so we also produced a CLUBBMICRO10 run that used this capability to run both schemes at 10 s. Because this run showed clear differences from the control, we produced a CLUBB-MICRO60 run where CLUBB and MG2 were substepped together at 60 s. Separately, we also produced a CLUBB10MICRO10 run, where the individual time steps for CLUBB and MG2 were reduced, but the two schemes were only coupled at the default rate of once per 300 s. To verify our prior belief that the model is less sensitive to the radiation time step size than to other physics time steps, we produced the ALLRAD10 run, which is identical to the ALL10 run except that the radiation is also run at a 10 second time step. Finally, we produced the ALL300 and ALL60 runs, which change dtime to 300 s and 60 s, respectively. ALL300 is useful as an additional control, because it decreases the dynamics-physics coupling time step, but does not decrease the CLUBB or MG2 time steps, nor does it decrease the dynamics time steps (except the remapping for the ver-

Name	Modified time steps	Step size	Run length
CTRL	None	N/A	38 mo
ALL10 ALL60 ALL300	Dynamics-physics coupling, dynamics time steps, land and sea ice model time steps, and all physics calculations except for updates to radiative transfer rates	10 s 60 s 300 s	38 mo 30 d 30 d
DYN10	All time steps in spectral element dynamical core	10 s	30 d
MICRO10	MG2 microphysics	10 s	30 d
CLUBB10	CLUBB unified cloud parameterization	10 s	30 d
CLUBB10MICRO10	CLUBB and MG2 (CLUBB+MG2 coupled using the 300 s default time step)	10 s	30 d
CLUBBMICRO10 CLUBBMICRO60	CLUBB+MG2 combined time step (CLUBB+MG2 coupled to each other every 10 s)	10 s 60 s	30 d 30 d
ALLRAD10	All time steps modified as in ALL10, except that radiative transfer rates are also updated every physics time step	10 s	30 d

Table 2. Runs performed using the default aerosol scheme.

tically Lagrangian advection scheme, which normally runs every 900 seconds). A summary of all these runs can be found in Table 2.

In EAMv1, the most important parameterization that does *not* have this built-in substepping capability is the ZM deep convection, which always runs at the time step given by dtime. In order to work around this limitation, we needed to modify the code and run simulations with a different model configuration. We describe these changes in section 3.3.

3 Results

3.1 Effects of Decreasing the Physics Time Step

Consistent with the literature on CAM, we find a 0.08 mm/d increase in global-mean total precipitation with 10 s time steps, mostly occurring at low latitudes. While convective precipitation decreases, large-scale precipitation increases by ∼60% in the tropics (defined here as latitudes from 30S to 30N), especially over land (Figure 2a). The overall effect is an increase in tropical precipitation over the Pacific warm pool, and a near-doubling of precipitation in parts of Borneo, New Guinea, and Colombia (Figure 2b). We also note an increase in heavy precipitation, seen in Figure 3 as a shift towards more precipitation falling in extreme precipitation events. This shift is again due primarily to an increase in heavy large-scale precipitation and a decrease in convective precipitation (not shown).

Evaporation must increase to fuel the precipitation increases. Over the oceans, this is due to slightly higher wind speed and lower near-surface relative humidity. The average 10 m wind speed in the tropics increases from 5.56 m/s to 5.70 m/s, and occurs mainly in the northern Indian ocean and central Pacific, while latent heat flux increases in the same areas, by about 4 W/m^2 (not shown). This is consistent with the CAM3 literature,

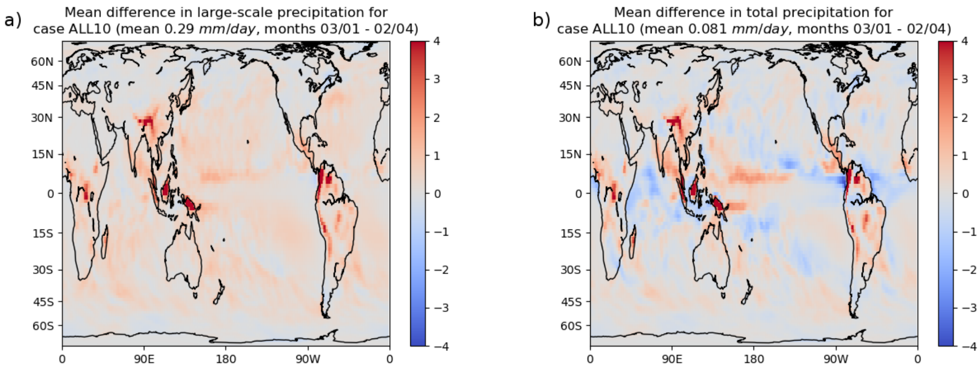

Figure 2. Changes in a) large-scale precipitation and b) total precipitation for the ALL10 run (ALL10 minus CTRL).

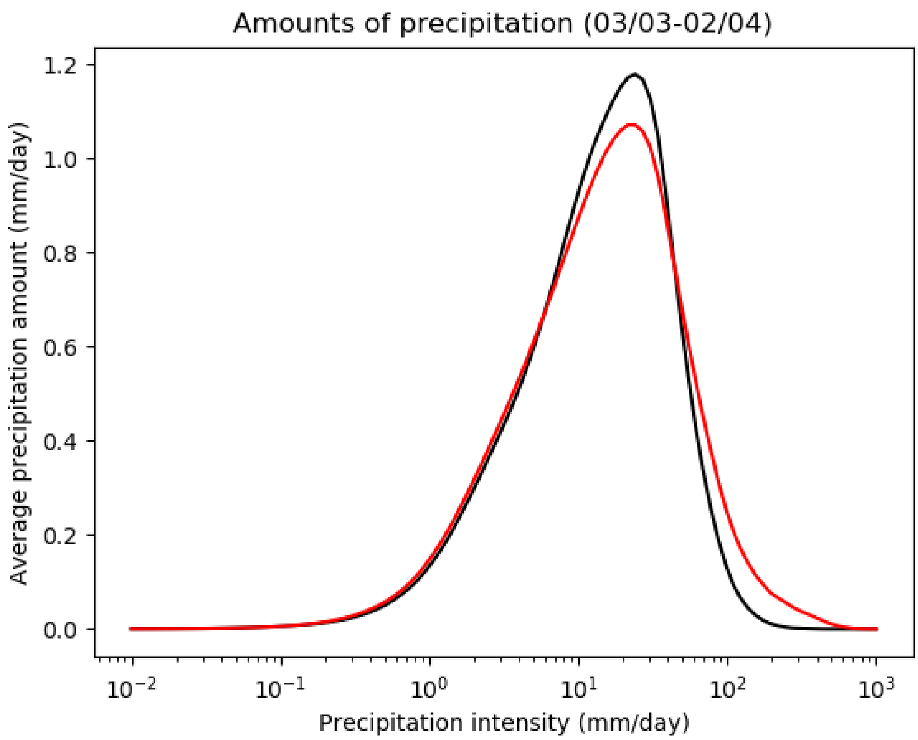

Figure 3. Global mean of the average amount of rain produced by precipitation falling at a given rate, produced from hourly data from CTRL (black) and ALL10 (red). Amount is normalized so that an integral over the natural logarithm of precipitation intensity yields total global mean precipitation amount. This plot only uses data from the final year of these simulation, as hourly data from previous years was not retained.

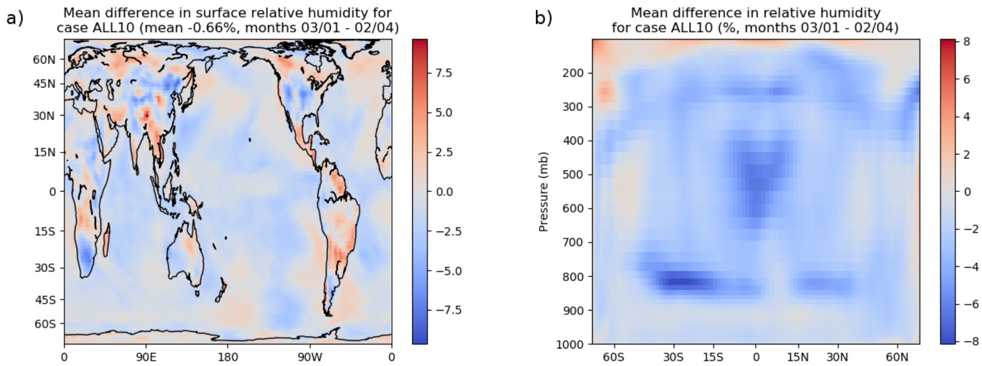

Figure 4. Changes in a) near-surface relative humidity and b) zonal mean relative humidity for the ALL10 run (ALL10 minus CTRL).

suggesting that an increase in wind speed contributes to an increase in evaporation for short time steps.

Unlike in CAM3, the relative humidity decreases throughout the troposphere in the ALL10 run, as shown in Figure 4. Since global mean precipitable water decreases while precipitation increases, the mean residence time of water in the atmosphere is reduced from about 7.3 days for CTRL, to 6.9 days for ALL10. Given that precipitation from the deep convection scheme is also reduced on average, this change can be most easily explained by dynamical changes that produce more large-scale condensation due to vapor convergence, or increased microphysical precipitation efficiency for a given condensation rate, or both.

The decreases in relative humidity in the 800-850 mb layer correspond to a significant reduction in low cloud mass (Figure 5). At the same time, we see an increase in cloud liquid above the boundary layer, particularly at high latitudes. In the ALL10 run, the cloud fraction also either decreases or remains unchanged nearly everywhere, except that the high cloud fraction (above 400 mb) increases over deep convective areas.

Consistent with the decrease in overall cloud mass and fraction, the ALL10 run shows substantially reduced radiative cloud forcing compared with CTRL, as can be seen in Figure 6. The effect on shortwave cloud forcing is especially large, the global mean being reduced from -43.0 W/m^2 to -37.5 W/m^2.

Spatial-pattern differences between CTRL and ALL10 are summarized by a Taylor diagram shown in Figure 7. We find that the effect of reducing the model time step to 10 seconds (black symbols) is comparable to the effect of doubling the model's horizontal grid spacing (red symbols), and much larger than differences due to interal variability of the model (green symbols). Historically, spatial resolution changes have been perceived as a major model change while accompanying time step changes have been taken for granted; Figure 7 illustrates that this viewpoint is incorrect. The variables most affected by the time step are related to precipitation, with the large-scale precipitation showing the most difference.

3.2 Effects of Changing the Physics Substepping

We did not have the computational resources to run all of our substepped configurations for multiple years, but many of the effects of substepping are quite large and can easily be distinguished with only a few days of data. In particular, all simulations

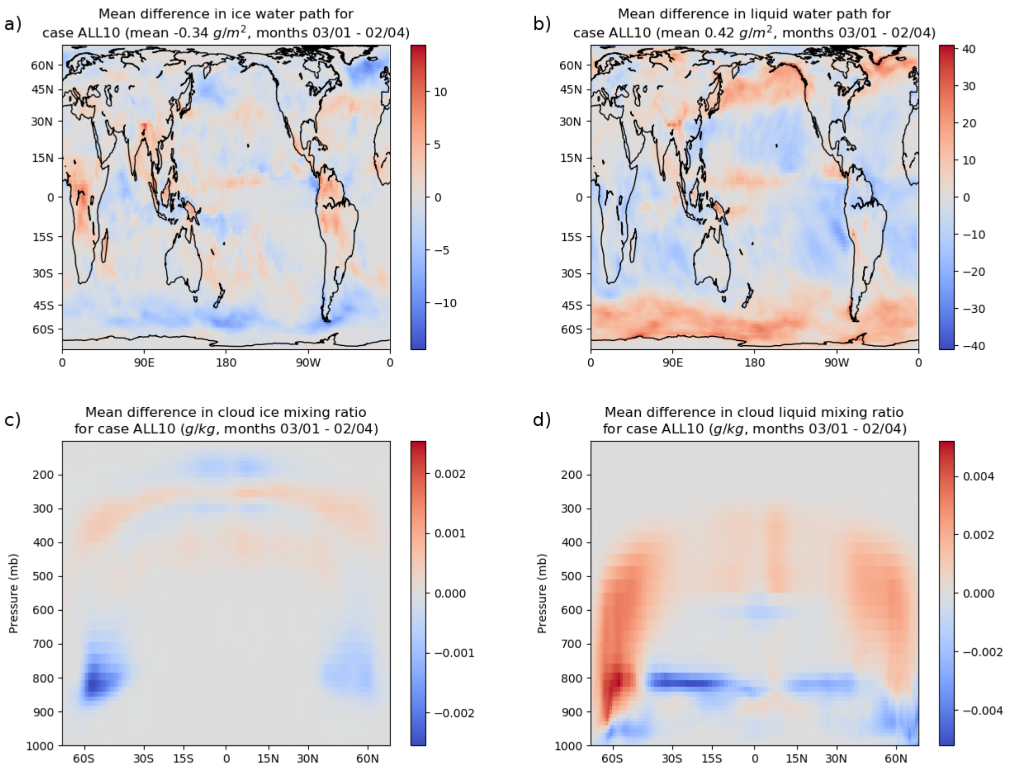

Figure 5. Changes in mass of cloud ice and liquid water for the ALL10 run (ALL10 minus CTRL), measured by a) ice water path, b) liquid water path, c) zonal mean cloud ice mixing ratio, and d) zonal mean cloud liquid mixing ratio.

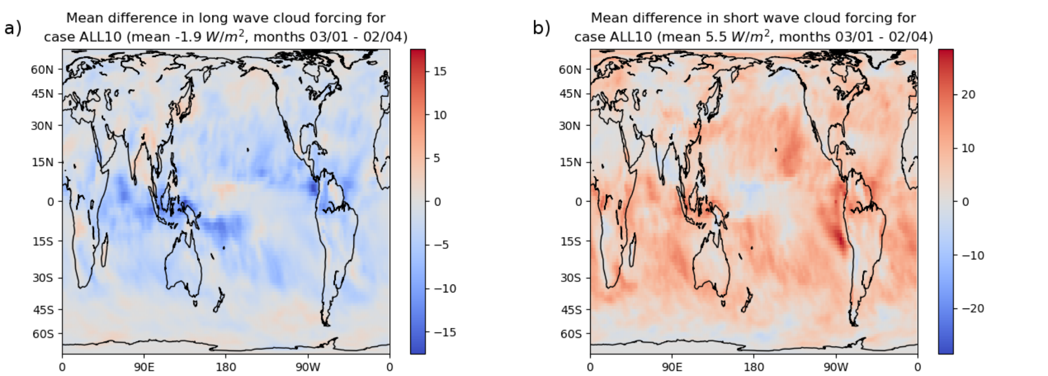

Figure 6. Changes in a) longwave cloud forcing and b) shortwave cloud forcing for the ALL10 run (ALL10 minus CTRL).

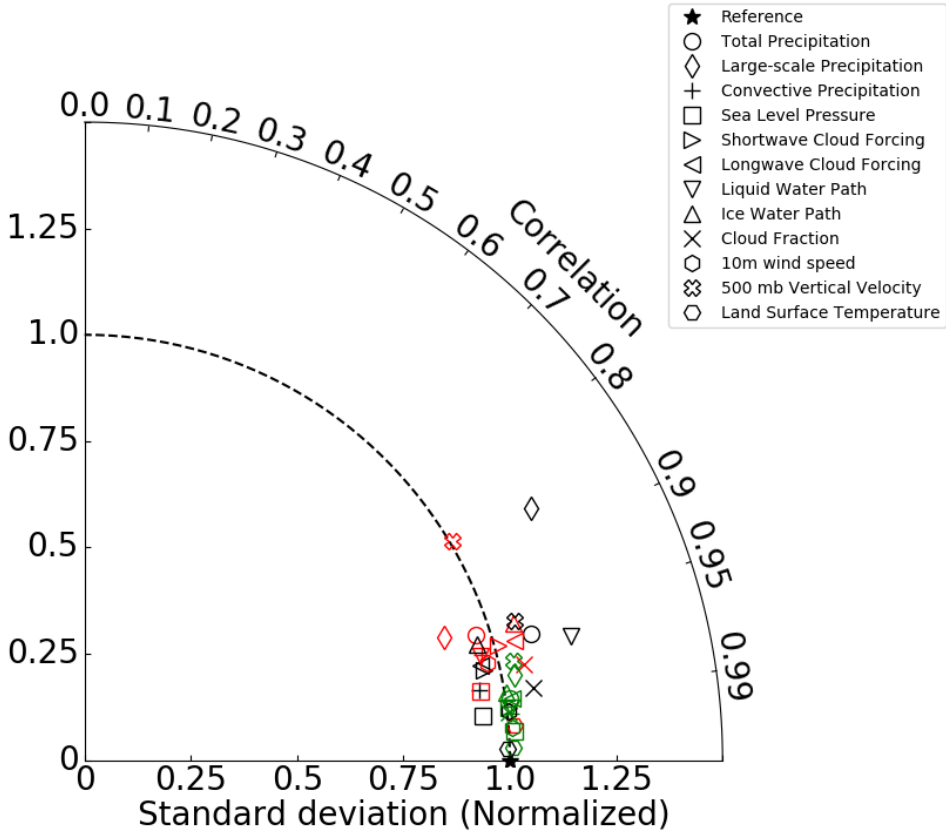

Figure 7. Taylor diagram comparing results from the CTRL and ALL10 runs (black), and comparing results from CTRL to a run with default settings using the ne16 grid (red), which has a grid spacing of $\sim 1.9^\circ$. From these runs, we use values averaged over a three year time period, starting March of the first simulated year. To show the typical variability of EAMv1, we also extend CTRL by an additional three years, and plot a comparison of those three years to the original three (green). Only spatial variability is accounted for in this diagram.

were initialized identically so differences between runs in the first ∼15 days is dominated by timestep differences rather than weather noise. Growth of weather noise over time is apparent in Figure 12, which provides the timeseries of global-average cloud-related radiative fluxes for all 30 days of simulation. The efficacy of using these first 15 days as a proxy for climatological mean differences is demonstrated in Table 3, which provides in parentheses in its 3rd and 5th column the difference between ALL10 and CTRL runs from 3 year and 15 day averages. Except for liquid water path and (to a lesser extent) latent heat flux, the 15 day average difference is an excellent estimate of the longer-term average. In the case of liquid water path, this is because the global mean is the sum of a decrease in the tropics and an increase over the rest of the globe; the decrease is slightly stronger in the 15 day run, while the increase is stronger in the 3 year run.

We first examine the changes in precipitation across these runs, shown in Figure 8. We can categorize our runs into five main categories based on large-scale precipitation:

1. The lowest average large-scale precipitation rates are found in CTRL, CLUBB10, and DYN10, suggesting that the cloud physics is not sensitive to the CLUBB or dynamics time steps.
2. A slightly higher large-scale precipitation rate is found in the ALL300 run, which has a reduced time step for the ZM deep convection and an increased dynamics-physics coupling frequency, but does not change the CLUBB or MG2 time steps. This run shows a mild repartitioning of precipitation from the convective to large-scale category.
3. The MICRO10 and CLUBB10MICRO10 runs show signs of increased precipitation efficiency overall, increasing both large-scale *and* total precipitation.
4. One of the largest large-scale precipitation rates comes from CLUBBMICRO10, which couples CLUBB to MG2 every 10 seconds, suggesting that an increase in CLUBB-MG2 coupling frequency has an additional effect beyond that from simply substepping MG2 more frequently. CLUBBMICRO60 may see a similar effect, though it is not as clearly distinguished from the MICRO10 run.
5. The ALL10, ALLRAD10, and ALL60 runs decrease both the dynamics-physics coupling time step and the time step used for all physics parameterizations, and these show the largest changes in precipitation.

While the increase in large-scale precipitation seen in the MICRO10 run is substantial, the spatial pattern is quite different from the ALL10 case. In particular, in the ALL10 case precipitation increases the most over tropical land. Table 4 shows that this large increase does not occur when CLUBB and/or MG2 are substepped by themselves, but only when both CLUBB and MG2 are substepped together, as in the CLUBBMICRO10 case.

We can also look at extreme precipitation, which we will categorize here as any precipitation falling at an hourly rate above 97.7 mm/d. Such high rates of precipitation are nearly absent from CTRL, but account for about 5% of the total precipitation in ALL10. Tables 3 and 4 show that this increase occurs mainly when the dynamics-physics coupling time step is changed, though some increase also occurs in CLUBBMICRO10.

Together, these results suggest that the main time steps affecting the precipitation are the MG2 microphysics time step and the coupling time step between the CLUBB and MG2 schemes. The change in the CLUBB and MG2 combined time step therefore explains most of the precipitation change noted earlier between the CTRL and ALL10 runs. Either the dynamics-physics coupling time step or the ZM deep convection time step could also be affecting the partitioning of precipitation between the convective and large-scale processes, since both of these time steps are changed in the ALL10 and ALL300 runs. We will investigate this further in section 3.3. The changes in total precipitation

Variable	CTRL (3 yr)	ALL10 (3 yr)	CTRL	ALL10	ALLRAD10	ALL60	ALL300	DYN10
Total precip. (mm/d)	3.10	3.18 (0.08)	2.82	2.87 (0.05)	2.89 (0.07)	2.90 (0.09)	2.84 (0.02)	2.82 (0.00)
Convective precip. (mm/d)	1.88	1.67 (-0.21)	1.65	1.44 (-0.21)	1.44 (-0.21)	1.50 (-0.15)	1.62 (-0.03)	1.64 (-0.01)
Large-scale precip. (mm/d)	1.21	1.50 (0.29)	1.17	1.43 (0.26)	1.44 (0.27)	1.41 (0.24)	1.22 (0.05)	1.18 (0.01)
Extreme precip. (mm/d)	0.05	0.16 (0.11)	0.03	0.15 (0.11)	0.15 (0.12)	0.11 (0.07)	0.07 (0.03)	0.03 (0.00)
Low-latitude land precip. (mm/d)	3.55	4.14 (0.59)	2.96	3.43 (0.47)	3.36 (0.41)	3.25 (0.29)	3.06 (0.10)	2.98 (0.02)
Precipitable water (kg/m^2)	22.7	22.0 (-0.7)	23.2	22.6 (-0.5)	22.6 (-0.5)	22.9 (-0.3)	23.2 (0.0)	23.2 (0.0)
Liquid water path (g/m^2)	46.6	47.0 (0.4)	49.9	49.8 (-0.1)	48.7 (-1.2)	52.1 (2.2)	53.5 (3.6)	49.6 (-0.3)
Low-latitude liquid water path (g/m^2)	37.8	34.2 (-3.6)	38.6	34.2 (-4.4)	33.6 (-5.0)	36.5 (-2.1)	38.9 (0.3)	38.5 (-0.1)
Ice water path (g/m^2)	10.3	9.9 (-0.3)	8.6	8.5 (-0.1)	8.5 (-0.1)	8.7 (0.1)	9.1 (0.5)	8.6 (0.0)
10 meter wind speed (m/s)	6.47	6.58 (0.11)	6.25	6.34 (0.10)	6.32 (0.07)	6.38 (0.13)	6.34 (0.09)	6.24 (0.00)
Lowest level relative humidity (%)	74.8	74.1 (-0.7)	77.0	76.4 (-0.6)	76.3 (-0.7)	76.7 (-0.3)	77.3 (0.3)	77.0 (0.1)
Latent heat flux (W/m^2)	89.6	91.9 (2.3)	76.1	76.8 (0.7)	77.0 (1.0)	78.1 (2.0)	76.8 (0.8)	76.0 (0.0)
Sensible heat flux (W/m^2)	19.6	18.6 (-1.0)	15.5	15.0 (-0.5)	15.2 (-0.3)	15.1 (-0.4)	15.9 (0.4)	15.6 (0.0)
Cloud fraction (%)	64.8	62.1 (-2.7)	65.3	62.9 (-2.4)	62.3 (-2.9)	64.1 (-1.2)	64.6 (-0.6)	65.1 (-0.2)
Low cloud fraction (%)	40.2	37.5 (-2.7)	42.9	40.4 (-2.5)	40.2 (-2.7)	40.9 (-2.0)	41.5 (-1.4)	42.6 (-0.3)
Mid-level cloud fraction (%)	26.4	25.1 (-1.3)	26.8	25.2 (-1.6)	25.1 (-1.7)	26.0 (-0.8)	26.9 (0.1)	26.7 (0.0)
High cloud fraction (%)	37.1	35.7 (-1.4)	35.7	35.4 (-0.2)	35.1 (-0.5)	36.7 (1.0)	36.9 (1.3)	35.7 (0.0)
Longwave cloud forcing (W/m^2)	22.9	21.0 (-1.9)	21.3	19.8 (-1.5)	19.6 (-1.6)	20.5 (-0.7)	21.1 (-0.2)	21.4 (0.1)
Shortwave cloud forcing (W/m^2)	-43.6	-38.1 (5.5)	-45.4	-40.1 (5.3)	-39.8 (5.6)	-42.1 (3.3)	-43.9 (1.5)	-45.2 (0.1)

Table 3. Global means of various variables in CTRL and all runs with changes to the dynamics-physics coupling or dynamics time steps. The first two columns contain averages over three years (starting in the third month), while all other columns contain averages over days 3-15 of the run. Extreme precipitation is defined as precipitation falling during an hour with an average rate over 97.7 mm/day. Low-latitude variables are averaged between 30S and 30N. Runs with reduced CLUBB+MG2 coupling time step are highlighted in purple. Numbers in parenthesis are differences from the equivalent time period from CTRL, but may not match differences in listed numbers due to rounding.

Variable	CTRL	ALL10	CLUBBMICRO10	CLUBBMICRO60	CLUBB10MICRO10	MICRO10	CLUBB10
Total precip. (mm/d)	2.82	2.87 (0.05)	2.90 (0.08)	2.87 (0.05)	2.87 (0.05)	2.86 (0.04)	2.84 (0.02)
Convective precip. (mm/d)	1.65	1.44 (-0.21)	1.54 (-0.11)	1.58 (-0.07)	1.58 (-0.07)	1.58 (-0.07)	1.66 (0.01)
Large-scale precip. (mm/d)	1.17	1.43 (0.26)	1.36 (0.19)	1.29 (0.13)	1.29 (0.12)	1.29 (0.12)	1.17 (0.00)
Extreme precip. (mm/d)	0.03	0.15 (0.11)	0.09 (0.05)	0.04 (0.01)	0.05 (0.01)	0.04 (0.01)	0.04 (0.00)
Low-latitude land precip. (mm/d)	2.96	3.43 (0.47)	3.32 (0.37)	3.24 (0.28)	2.93 (-0.03)	2.90 (-0.06)	2.96 (0.00)
Precipitable water (kg/m^2)	23.2	22.6 (-0.5)	22.7 (-0.5)	22.9 (-0.3)	23.1 (-0.1)	23.1 (-0.1)	23.2 (0.0)
Liquid water path (g/m^2)	49.9	49.8 (-0.1)	45.7 (-4.2)	46.9 (-3.0)	46.8 (-3.0)	47.4 (-2.5)	49.3 (-0.6)
Low-latitude liquid water path (g/m^2)	38.6	34.2 (-4.4)	33.8 (-4.9)	35.6 (-3.0)	36.2 (-2.5)	38.2 (-0.4)	
Ice water path (g/m^2)	8.6	8.5 (-0.1)	8.5 (-0.1)	8.6 (0.0)	9.6 (0.9)	9.6 (1.0)	8.6 (0.0)
10 meter wind speed (m/s)	6.25	6.34 (0.10)	6.27 (0.02)	6.23 (-0.01)	6.26 (0.01)	6.27 (0.02)	6.26 (0.01)
Lowest level relative humidity (%)	77.0	76.4 (-0.6)	76.3 (-0.7)	76.6 (-0.4)	76.5 (-0.5)	76.4 (-0.6)	76.9 (0.0)
Latent heat flux (W/m^2)	76.1	76.8 (0.7)	77.7 (1.6)	77.1 (1.0)	77.3 (1.3)	77.3 (1.2)	76.6 (0.5)
Sensible heat flux (W/m^2)	15.5	15.0 (-0.5)	15.0 (-0.6)	15.1 (-0.4)	15.4 (-0.2)	15.0 (-0.6)	15.7 (0.2)
Cloud fraction (%)	65.3	62.9 (-2.4)	64.3 (-1.0)	64.6 (-0.6)	65.6 (0.3)	65.2 (0.0)	65.4 (0.2)
Low cloud fraction (%)	42.9	40.4 (-2.5)	42.9 (0.0)	42.8 (-0.1)	43.0 (0.1)	42.7 (-0.2)	43.1 (0.2)
Mid-level cloud fraction (%)	26.8	25.2 (-1.6)	25.6 (-1.2)	26.2 (-0.6)	26.8 (0.0)	26.7 (-0.1)	26.6 (-0.1)
High cloud fraction (%)	35.7	35.4 (-0.2)	34.8 (-0.9)	35.2 (-0.5)	36.3 (0.6)	36.2 (0.5)	36.0 (0.3)
Longwave cloud forcing (W/m^2)	21.3	19.8 (-1.5)	20.2 (-1.0)	20.7 (-0.6)	21.8 (0.5)	21.9 (0.6)	21.2 (-0.0)
Shortwave cloud forcing (W/m^2)	-45.4	-40.1 (5.3)	-42.8 (2.6)	-43.9 (1.5)	-45.5 (-0.1)	-45.3 (0.1)	-45.6 (-0.2)

Table 4. As in Table 3, but only averaging days 3-15 and including runs with changes to CLUBB or MG2 time steps. Runs with reduced CLUBB+MG2 coupling time step are highlighted in purple, and runs with reduced MG2 time step with *no* change to the CLUBB+MG2 coupling time step are highlighted in red.

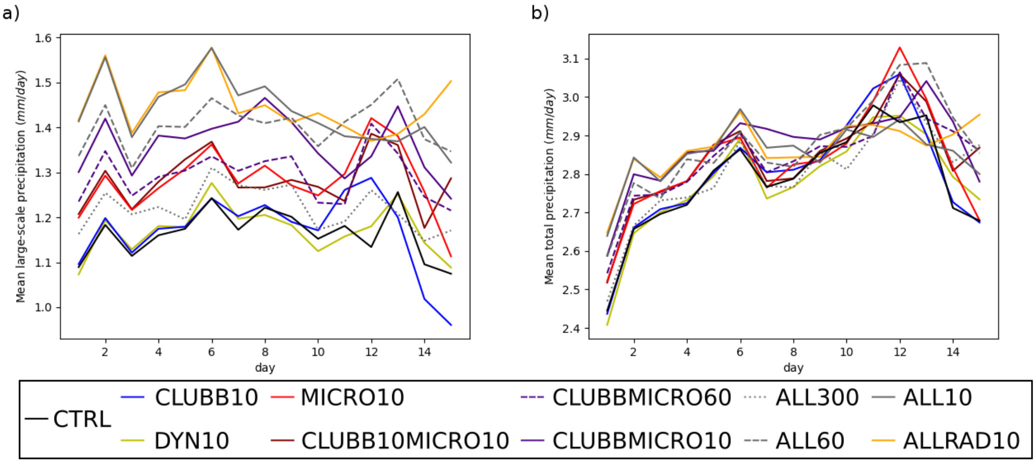

Figure 8. Daily global means of a) large-scale precipitation only and b) total precipitation for substepped runs.

are mostly apparent for the first week of the run, after which the runs with default MG2 time step see a significant increase in convective precipitation (not shown), leading to no systematic difference between simulations after this point.

The "drying" of the atmosphere that occurs in the ALL10 run also appears in the CLUBBMICRO10 run, but is relatively weak in the MICRO10 run, as can be seen in the precipitable water in Table 4. As shown in Figure 9, the cloud liquid in the CLUBBMICRO10 run only matches the ALL10 run at low altitudes, while the ALL300 run is much more effective at matching ALL10 at higher altitudes, suggesting that the dynamics-physics coupling time step is responsible for these increases in cloud liquid. (In the next section we will see that the ZM time step is not likely to be the cause, since this increase in cloud liquid is not seen in the CLD10PA run shown in Figure 13.) CLUBBMICRO10 and CLUBBMICRO60 also consistently produce clouds in the lowest level of the atmosphere over land, particularly in South America and Southeast Asia, which are not seen in any other run.

Wan, Zhang, Rasch, et al. (2020) also saw a reduction in cloud fraction when the dynamics-physics coupling time step was reduced. In one of the simulations in that study (labeled "v1_Dribble"), the coupling of the rest of the model to CLUBB+MG2 was adjusted by "dribbling" the effects of all other processes into the CLUBB+MG2 loop, rather than applying those effects to the initial CLUBB+MG2 input state. This simulation emulates the effect of decreasing the dynamics-physics coupling time step on the CLUBB and MG2 parameterizations, without changing the time steps themselves. In this test, the effects of the dynamics and radiation are applied more gently to the state seen by CLUBB, and in particular, CLUBB's input state is influenced more mildly by radiative cooling (Wan, Zhang, Yan, et al., 2020). In some regions this results in a more convective boundary layer, and to a reduction in mean cloud fraction and liquid water path. This mechanism may partially explain why increasing the dynamics-physics coupling frequency (and hence the CLUBB-radiation coupling frequency) leads to a lower cloud fraction in our simulations as well.

The overall differences in ice and liquid water path are shown in Figure 10. We see that, in the tropics, the runs with reduced MG2 time step reduce the liquid water path in a way that is similar to the ALL10 run, while the ALL300 run increases the ice and liquid water path everywhere. We also note that if MG2 is substepped independently

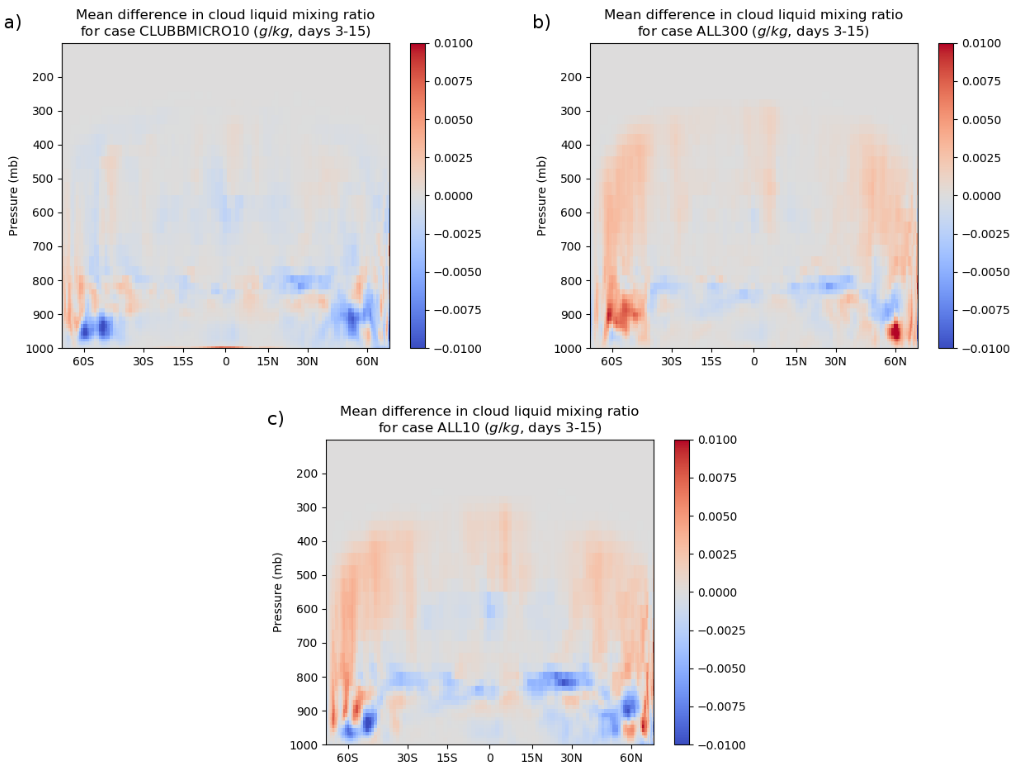

Figure 9. Differences in zonal mean cloud liquid mixing ratio versus CTRL for a) ALL300, b) CLUBBMICRO10, and c) ALL10.

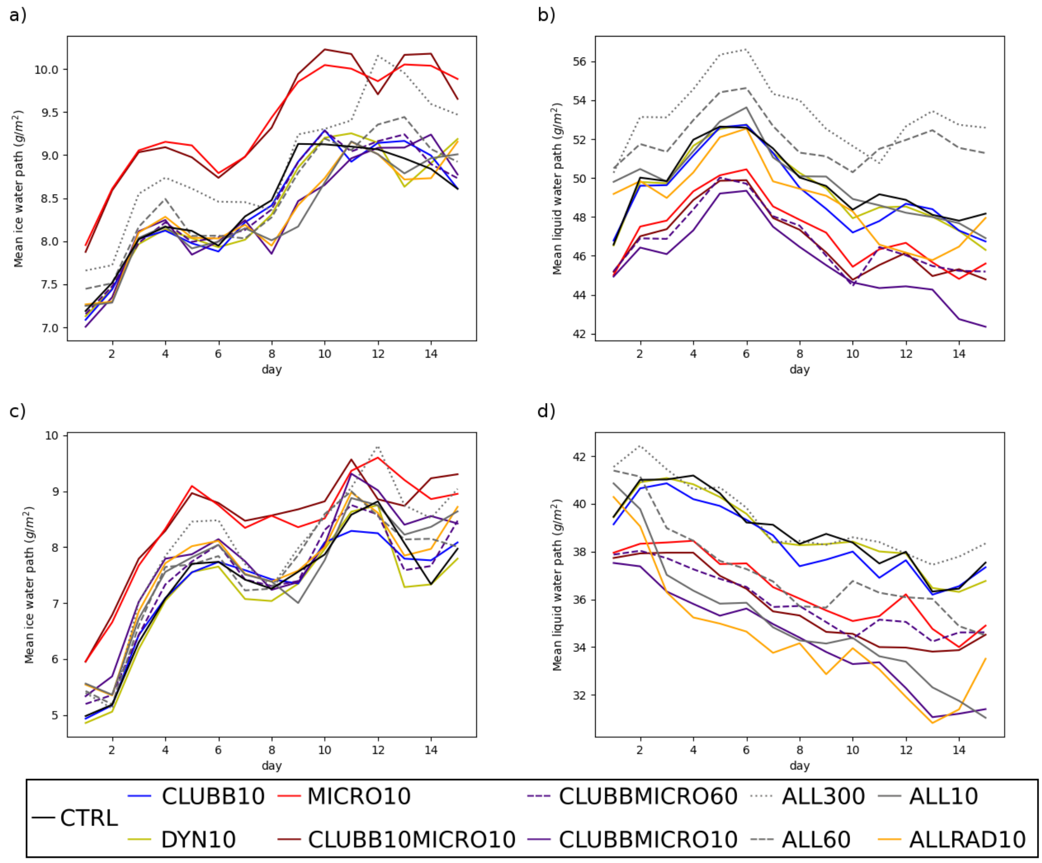

Figure 10. Daily means for a,c) ice water path and b,d) liquid water path for substepped runs. Plots a-b) show global means, while c-d) show means over low latitude grid points (30S–30N).

from CLUBB, the ice water path (and high cloud fraction, as seen in Table 4) increase significantly, but this does not occur when MG2 and CLUBB are substepped together.

We saw earlier that the ALL10 run caused a reduction in cloud fraction throughout most of the atmosphere, especially in the low cloud fraction. As shown in Figure 11, this effect seems to have different causes, depending on which level of the atmosphere is examined. Reductions in low cloud are primarily due to the reduction in the dynamics-physics coupling substep, but the CLUBB and MG2 combined time step has a greater effect on the cloud fraction above 700 mb.

Finally, we turn to the changes in radiative cloud forcing between runs. The magnitudes of both shortwave and longwave cloud forcing are reduced in the ALL10, ALLRAD10, CLUBBMICRO10, and CLUBBMICRO60 runs, likely due to the significant decreases in cloud fraction and liquid water path found in the tropics. The MICRO10 and CLUBB10MICRO10 runs, on the other hand, have a much larger ice water path, leading to an increase in longwave cloud forcing. The ALL300 run has both a reduced low cloud fraction and an increase in liquid and ice water path, leading to a decrease in shortwave cloud forcing and no net change in longwave cloud forcing.

We notice that most variables take a few days for the differences between runs to fully develop, but the effect of a change in the MG2 time step strongly affects large-scale

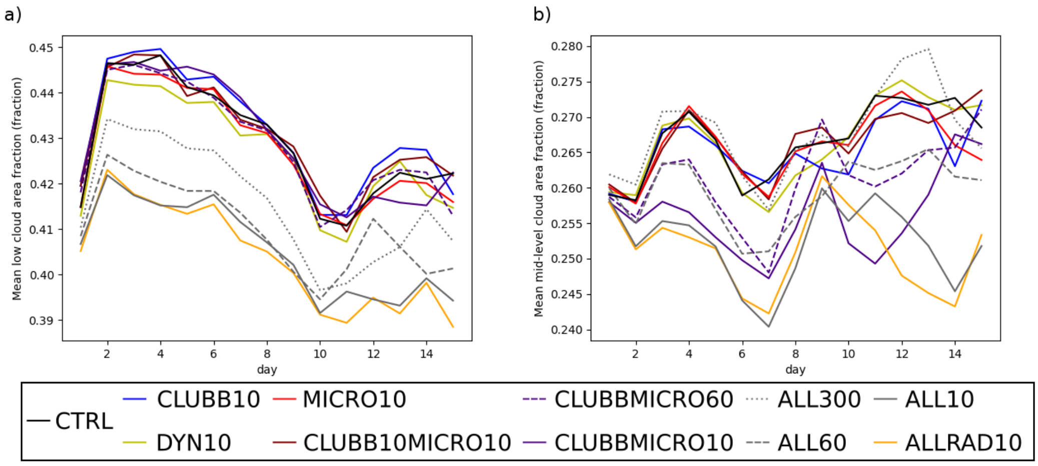

Figure 11. Daily global means of a) low cloud fraction (> 700 mb), and b) mid-level cloud fraction (400-700 mb) for substepped runs.

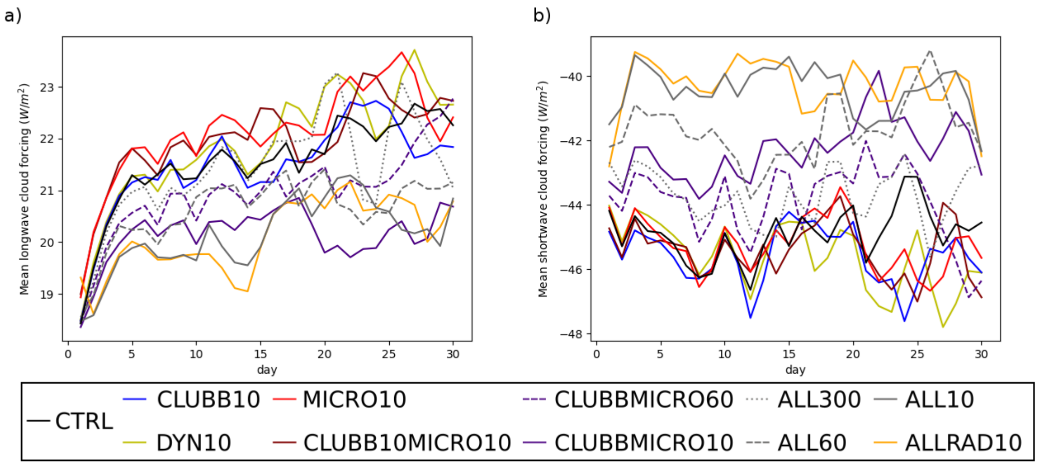

Figure 12. Daily global means of a) longwave cloud forcing and b) shortwave cloud forcing for substepped runs.

Name	Substepped processes	Substep size	Run length
CTRLPA	None	N/A	30 d
ALL10PA	All time steps modified as in ALL10.	10 s	30 d
CLUBBMICRO10PA	CLUBB+MG2 combined loop	10 s	30 d
ZM10PA	ZM deep convection	10 s	30 d
CLUBBMICRO10ZM10PA	CLUBB+MG2 combined time step and ZM deep convection (CLUBB+MG2 coupled to each other every 10 s, and to ZM using the 1800 s default)	10 s	30 d
CLD10PA	CLUBB+MG2+ZM combined time step (all three parameterizations coupled every 10 s)	10 s	30 d

Table 5. Runs performed using prescribed aerosols

precipitation and ice water path within the first day. We suspect that most effects of a decreased time step require a certain degree of "spin up" in order for runs starting with the same initial condition to become more distinct. We hypothesize that the more instantaneous changes are primarily due to the direct effects of a decreased time step on microphysical process rates, which can respond directly and dramatically to changes in time step (Santos et al., 2020).

3.3 Substepping the ZM Deep Convection Scheme

So far, we have been unable to distinguish between the effect of substepping the ZM deep convection scheme and the effect of reducing the dynamics-physics coupling time step. In order to explore the effect of ZM substepping on results, we produced a set of code modifications to EAMv1 to allow this scheme to be substepped on its own. Most of these changes were simple, but we never managed to get coupling between ZM and the MAM4 modal aerosol scheme to work properly. Ultimately, we resorted to using EAM's prescribed aerosol capability (Lebassi-Habtezion & Caldwell, 2015) for substepped-ZM runs. This required switching to a configuration where prescribed aerosol data was available, so we used a present-day configuration (E3SMv1 compset FC5AV1C-04P2). As a result, these results cannot be directly compared to our previous runs, though we used the same spatial grid, and the physics of this compset is similar to our previous runs, aside from initial/boundary conditions. We first reproduced the CTRL, ALL10, and CLUBBMICRO10 runs using prescribed aerosols, and added a run that substeps ZM by itself. We then produced a run that substeps both ZM and CLUBB+MG2 at 10 seconds, while only coupling ZM to CLUBB+MG2 at the default 1800 second time step. Finally we produced a run that substeps and couples ZM, CLUBB, and MG2 together using a 10 second time step. These simulations are summarized in Table 5. We append "PA" to run names to indicate that they use prescribed aerosols. Aside from the choice of compset and use of prescribed aerosols, CTRLPA is configured identically to CTRL, ALL10PA to ALL10, and CLUBBMICRO10PA to CLUBBMICRO. Global means of selected variables for all -PA runs are shown in Table 6.

First, by looking at the large-scale precipitation in Table 6, we can see that the CLD10PA run, which substeps the ZM deep convection along with CLUBB and MG2 in a single loop, has almost the same partitioning of precipitation as seen in the ALL10PA run. This

Variable	CTRLPA	ALL10PA	CLD10PA	CLUBBMICRO10ZM10PA	CLUBBMICRO10PA	ZM10PA
Total precip. (mm/d)	2.89	2.92 (0.03)	2.94 (0.04)	2.95 (0.06)	2.92 (0.02)	2.90 (0.00)
Convective precip. (mm/d)	1.71	1.48 (-0.23)	1.51 (-0.20)	1.57 (-0.14)	1.58 (-0.13)	1.69 (-0.01)
Large-scale precip. (mm/d)	1.19	1.44 (0.26)	1.43 (0.24)	1.38 (0.20)	1.34 (0.15)	1.21 (0.02)
Extreme precip. (mm/d)	0.04	0.16 (0.12)	0.12 (0.08)	0.09 (0.05)	0.07 (0.02)	0.04 (0.00)
Low-latitude land precip. (mm/d)	2.86	3.40 (0.54)	3.27 (0.42)	3.34 (0.48)	3.22 (0.36)	2.92 (0.06)
Precipitable water (kg/m^2)	23.5	23.0 (-0.6)	23.0 (-0.5)	23.1 (-0.4)	23.0 (-0.5)	23.6 (0.1)
Liquid water path (g/m^2)	47.7	46.1 (-1.6)	42.2 (-5.6)	42.7 (-5.1)	43.6 (-4.1)	46.6 (-1.1)
Low-latitude liquid water path (g/m^2)	39.0	34.2 (-4.7)	31.9 (-7.1)	32.3 (-6.7)	33.7 (-5.3)	37.9 (-2.0)
Ice water path (g/m^2)	9.8	9.2 (-0.6)	8.7 (-1.1)	8.5 (-1.3)	9.4 (-0.4)	9.0 (-0.8)
10 meter wind speed (m/s)	6.34	6.32 (-0.01)	6.27 (-0.07)	6.31 (-0.03)	6.24 (-0.10)	6.34 (0.00)
Lowest level relative humidity (%)	76.6	76.1 (-0.5)	76.0 (-0.6)	76.0 (-0.6)	76.2 (-0.4)	76.6 (0.0)
Latent heat flux (W/m^2)	79.0	79.2 (0.2)	79.7 (0.7)	80.3 (1.3)	79.0 (0.0)	79.4 (0.4)
Sensible heat flux (W/m^2)	15.7	15.0 (-0.8)	15.2 (-0.6)	14.9 (-0.8)	15.2 (-0.5)	15.6 (-0.2)
Cloud fraction (%)	65.6	62.7 (-2.9)	63.9 (-1.7)	64.4 (-1.1)	64.4 (-1.2)	65.4 (-0.1)
Low cloud fraction (%)	42.9	40.9 (-2.0)	42.3 (-0.6)	43.0 (0.1)	43.1 (0.2)	42.6 (-0.3)
Mid-level cloud fraction (%)	26.6	24.8 (-1.8)	25.0 (-1.6)	25.1 (-1.5)	25.2 (-1.4)	26.5 (-0.1)
High cloud fraction (%)	36.3	34.9 (-1.4)	34.7 (-1.6)	35.1 (-1.3)	34.9 (-1.4)	36.4 (0.1)
Longwave cloud forcing (W/m^2)	20.6	18.2 (-2.4)	19.1 (-1.5)	19.3 (-1.4)	19.3 (-1.3)	20.4 (-0.2)
Shortwave cloud forcing (W/m^2)	-45.8	-39.5 (6.3)	-41.9 (3.9)	-42.5 (3.3)	-42.9 (2.9)	-45.3 (0.5)

Table 6. Global means of various variables in prescribed aerosol runs. All columns contain averages over days 3-15 of the run. Extreme precipitation is defined as precipitation falling during an hour with an average rate over 97.7 mm/day. Low-latitude land precipitation is an average over land between 30S and 30N. Runs with reduced CLUBB+MG2 coupling time step are highlighted in purple. Numbers in parenthesis are differences from CTRLPA, but may not match differences in listed numbers due to rounding.

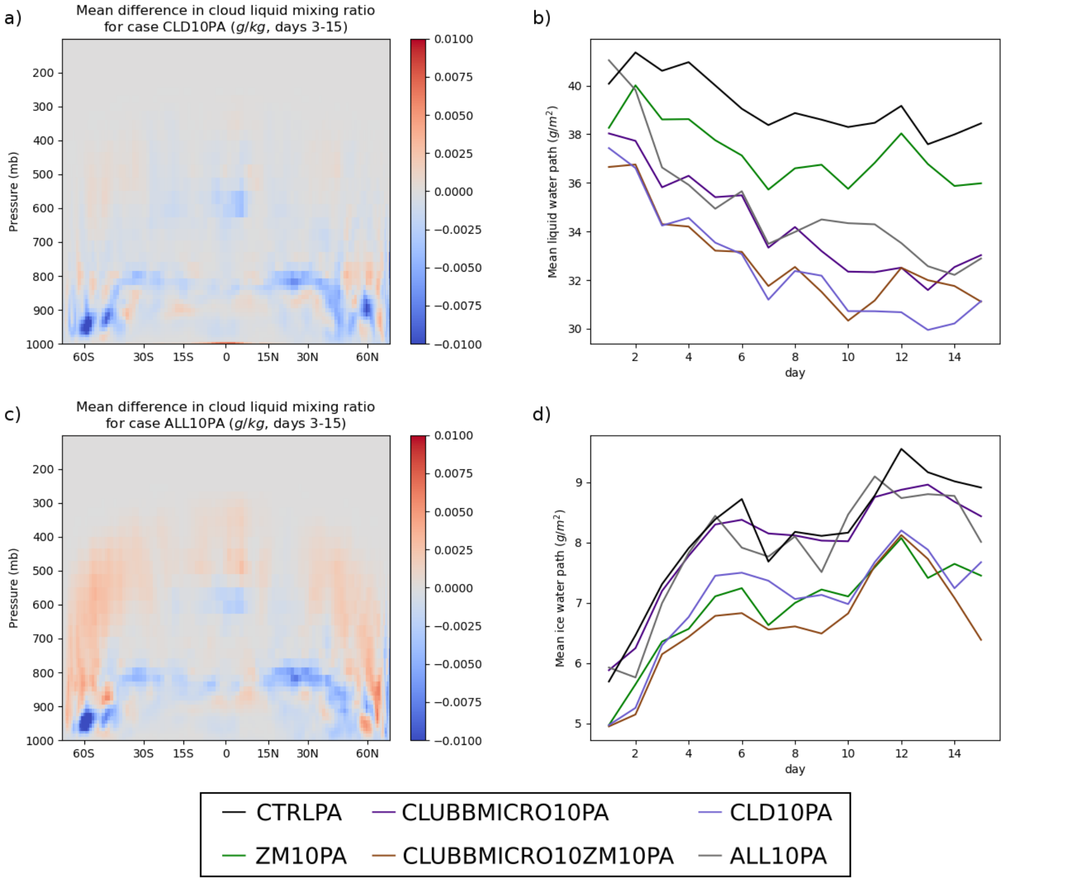

Figure 13. Left: Differences in zonal mean cloud liquid mixing ratio versus CTRLPA for a) CLD10PA and c) ALL10PA. Right: Daily means over low latitudes (30S–30N) for prescribed aerosol substepped runs of b) liquid water path, and d) ice water path.

suggests that the partitioning of precipitation between convective and stratiform parameterizations is mostly affected by the time steps of the physics parameterizations and the coupling between them. It is much less influenced by the dynamics-physics coupling time step. We also see that substepping ZM by itself has almost no impact on convective precipitation, while tightening the CLUBB+MG2+ZM coupling has a large effect.

Next, we note that deep convection substepping, like substepping of the other parameterizations, causes a decrease in low cloud liquid mass, and contributes to the overall pattern seen in the ALL10PA run. This is seen in Figure 13, where the distribution of liquid water below 750 mb is quite similar between the CLD10PA run and the ALL10PA run. However, the increase in cloud liquid above this level is still absent from the CLD10PA run, implying that that increase requires more frequent dynamics-physics coupling to occur. This means that the CLD10PA "overshoots" the ALL10PA run in the tropics, having an even lower liquid water path. Unlike the effect of ZM substepping on precipitation, the effect on cloud liquid does not rely on coupling with CLUBB and MG2, since the CLUBBMICRO10ZM10PA run and the CLD10PA run have fairly similar liquid water path. Similarly, substepping ZM causes a reduction in ice water path regardless of its coupling with CLUBB and MG2, but the ice water path recovers if the dynamics-physics coupling time step is also reduced.

Other than this, ZM substepping accounts for very little of the differences between the CTRLPA and ALL10PA runs, as can be seen in the lower portions of Table 6. ZM substepping does not substantially affect cloud fraction, and its effects on both longwave and shortwave cloud forcing are relatively small compared with the effect of changing the CLUBB and MG2 combined time step or the dynamics-physics coupling time step.

4 Physical Insights

We have found that reducing EAMv1's time step has a number of effects on model climate, and by adjusting the model substepping, we have attributed those effects to the time step sensitivity of particular processes or coupling intervals. In this section, we offer a number of potential explanations for these effects, which may be the basis for further research on the model's time step sensitivity.

4.1 Time Discretization in a Sequential-Split System

Liquid water path in EAMv1 is written out directly after the microphysics has run (Donahue & Caldwell, 2018). During the first CLUBB+MG2 substep after the dynamics has run, CLUBB is often reacting to a highly supersaturated state, and it produces a large amount of condensate, much of which is then removed by MG2 (Wan, Zhang, Yan, et al., 2020). In subsequent CLUBB+MG2 substeps, CLUBB produces relatively little condensate, and MG2 continues to remove more cloud liquid. Thus the model contains far more cloud liquid immediately after the first CLUBB substep than after all CLUBB+MG2 substeps have run. Reducing the CLUBB+MG2 combined time step does not change this situation, because the burst of additional cloud liquid is always produced by CLUBB during the first substep after the dynamics runs, and is not a response to the microphysics. When the dynamics-physics coupling time step is reduced, however, the effect of the dynamics is introduced to CLUBB+MG2 more gradually, rather than producing one large burst of condensate at 1800 second intervals. As a result, MG2 removes a smaller fraction of this new cloud liquid, and more is observed at the point in the time step where the liquid water path is output.

This situation is analogous what we saw in the simple model (Figure 1b), but applied to cloud liquid rather than supersaturation. The liquid water path varies significantly within each physics time step, but since we record the liquid water content after MG2 runs, we are systematically measuring values near the low end of this range. If the time step is reduced, the liquid water content varies within a narrower range for each time step, and so the values we record from that range must increase. We believe that this accounts for the increase in liquid water content that occurs in much of the atmosphere when the dynamics-physics coupling time step is reduced, as seen in Figures 5(d) and 9(b-c). However, this does not explain the *reduction* in cloud liquid seen at lower altitudes, which must be the result of different mechanisms (e.g. the microphysical process rate changes discussed below).

To test this explanation for the effect of dynamics-physics coupling on cloud liquid, the liquid water content could be recorded at several points during each time step, to see how the full range of possible output values depends on the time step. Alternately, the coupling between the dynamics, CLUBB, and MG2 could be modified to avoid producing large bursts of liquid at 1800 second intervals, to see if this reduces the time step sensitivity of liquid water content. In fact, the authors of Wan, Zhang, Rasch, et al. (2020) appear to have performed both of these types of experiment (Wan, Zhang, Yan, et al., 2020), though they have not yet published details of their findings on liquid water content specifically.

We believe that sequential coupling errors are also partly responsible for the decrease in convective precipitation at shorter time steps, due to an effect described by Williamson

(2013). When dynamics produces supersaturation in an atmospheric column, the ZM scheme competes with CLUBB+MG2 to remove that supersaturation. Since ZM runs first each time step, it is able to produce precipitation before CLUBB+MG2 remove supersaturation from the atmosphere, giving the deep convection an advantage. However, if the model time step is reduced, or if ZM is substepped with CLUBB+MG2 (as in our CLD10PA run), ZM will operate on an input state that is on average more similar to the state of the atmosphere immediately after MG2 runs, i.e. a state with much less supersaturation and less precipitable water generally. It then produces less convective precipitation in response, leaving stratiform precipitation to pick up the slack.

This mechanism could be tested by swapping the order of ZM and the CLUBB+MG2 loop in the model. If the convective precipitation is easily affected by competition for supersaturation with CLUBB, running CLUBB first during every time step should cause a significant repartitioning of precipitation from the convective to large-scale categories.

4.2 Changes to Microphysical Process Rates

Our past research on the MG2 microphysics identified rain evaporation and self-collection as processes that were poorly resolved by MG2's default time step of 300 seconds (Santos et al., 2020). Zheng et al. (2020) evaluated EAMv1's performance for precipitating marine stratocumulus clouds using data from the ARM MAGIC campaign, and found that the vertical profile of rain evaporation depended strongly on the time step used for MG2. At a 300 second time step, the evaporation rate had a large peak near the surface, while at a 30 second time step, the peak evaporation rate occurred near the cloud base and was only half as large.

With this in mind, we can consider the effect of a dramatic reduction in large-scale rain evaporation rate, especially near the model's surface. This would produce a drier, warmer boundary layer, along with an increase in the amount of rain that reaches the surface. Latent heat flux from the surface would then increase, while sensible heat flux would decrease, partially compensating for the effect of the reduced rain evaporation rate. This matches the pattern seen in the global means in Tables 3, 4, and 6, since in every case where the MG2 time step is reduced (columns highlighted in purple or red), the large-scale precipitation and latent heat flux increase, while the relative humidity in the lowest level of the atmosphere and the sensible heat flux decrease.

Since the decrease in rain evaporation is stronger than the increased surface moisture flux, the precipitable water also decreases. This could partially explain both the reduction in liquid water path and the reduction in convective precipitation in runs where MG2 is substepped. (Less large-scale precipitation would be produced as well, but more of it would reach the surface due to the reduced evaporation rate.)

We have performed some tests using a modified precipitation fraction method as in Zheng et al. (2020), which has the primary effect of increasing the fraction of precipitation that evaporates before reaching the surface. Preliminary results appear to support our hypothesis, since in many ways increasing the evaporation rate has the opposite effect from reducing the MG2 time step. In particular, we see a significant decrease in total precipitation, a shift of precipitation from the large-scale to convective schemes, and increases in precipitable water and liquid water path (not shown).

4.3 Grid-Point Storms and Resolved Convection

In order to gain a better understanding the extreme precipitation events that occur in the ALL10 run, we looked for such a case study that occurs early in our simulations, and thus can be compared across all runs. One such event occurs in South America in the Guiana Highlands (6°N 67°W) on the first simulated day, with the ALL10 run sustaining a precipitation of over 215 mm/d between 0900 and 0430 local time, peaking

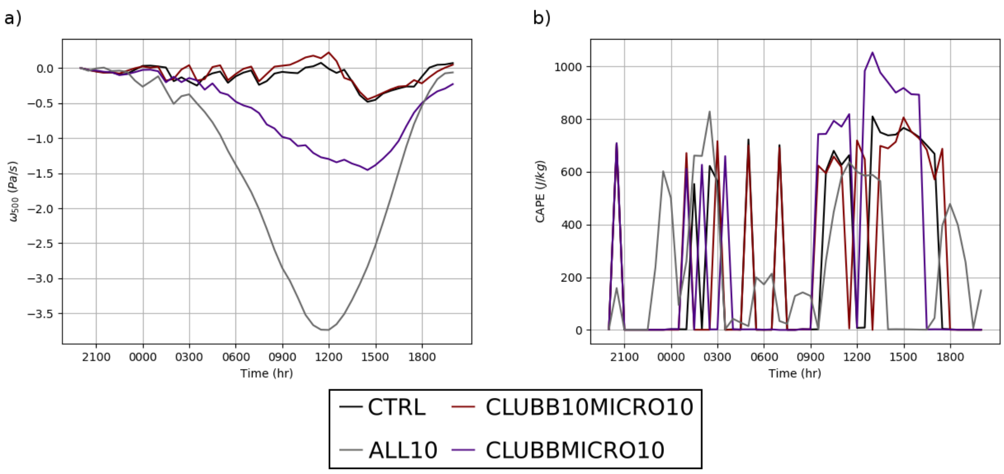

Figure 14. First day time series of a) 500 mb vertical velocity and b) CAPE for an atmospheric column producing heavy precipitation. Horizontal axis shows local time (UTC-4:00).

at about 323 mm/d (compared to a range of 104–152 mm/d in CLUBBMICRO10, and a range of 17–65 mm/d in CTRL). In the ALL10 run, this storm resembles the grid-point storms described by Williamson (2013), with explosive growth in vertical velocity, moisture convergence, and condensation. Figure 14a) shows vertical velocity at 500 mb (ω_{500}) over time for a particular column in this storm. We show only a small number of simulations to demonstrate the effects of CLUBB+MG2 coupling time step and the dynamics-physics coupling time step have large effects on vertical velocity on this case. However, our results from other simulations show any pair of cases with the same CLUBB+MG2 coupling time step and dynamics-physics coupling time step have the same total precipitation to within a few percent over this time period, with essentially no role played by any of the other changes made in our study (including the ZM substepping).

We have no diagnostics designed to identify and count these grid-point storms in longer runs, but there is circumstantial evidence that they are more common when using small time steps. We can see that there is much more extreme precipitation in cases with a reduced CLUBB+MG2 time step and/or reduced dynamics-physics coupling time step (Figure 3 and Tables 3, 4 and 6), and for the first few days of simulations, the largest precipitation events in ALL10 are consistently associated with values of ω_{500} that are much larger than any occurring in CTRL, with heavy precipitation occurring over only a few grid cells wide.

While the role of CLUBB+MG2 coupling is still unclear, we are aware of two explanations for why such grid point storms may grow more easily when the dynamics-physics coupling time step is smaller. According to Williamson (2013), using a shorter time step weakens the parameterized convection schemes, particularly when the time step is much shorter than the scheme's relaxation timescale. The ZM scheme is therefore relatively incapable of removing CAPE, which is persistently high in grid-point storms. The large-scale condensation scheme is exposed to an unrealistic level of supersaturation, and the model responds to the absence of parameterized convection by entering a "vicious cycle" where the condensation releases excessive heat, producing stronger ascent, which causes increased horizontal convergence to draw in even more moisture to condense. The lack of parameterized convection thus results in more vertical motion at the resolved scale.

Herrington and Reed (2017) also suggests that the release of latent heat produced by the condensation scheme directly forces resolved-scale convection, and further notes that the consumption of CAPE through resolved-scale vertical motion in the dynamics can inhibit the deep convection scheme, at least when using CAM4 at a high horizontal resolution. Enhanced resolved-scale convection can therefore *cause* the parameterized convection to become weaker, as well as *being caused by* weak parameterized convection. Herrington and Reed (2018) examines the dynamics-physics coupling time step as well as horizontal resolution for an idealized test case, and finds that coarse time steps are unable to properly resolve the rapid growth in vertical velocity that arises from the positive feedback loop between the dynamics and condensation scheme, especially (but not exclusively) at higher resolutions. This form of time step sensitivity occurs even when using a very simple moist physics model with no parameterized convection at all.

Intense grid-scale storms in EAMv1 can therefore become more common at short time steps either due to a weakening of the ZM parameterized convection, or due to better resolution of the dynamics-CLUBB feedback loop that drives resolved-scale convection. Both of these mechanisms probably occur to some extent, but the increase in resolved-scale convection seems to be more relevant for the grid-point storm in our case study. Consider Figure 14b), which shows CAPE calculated from the atmospheric state passed to ZM. If ZM was simply failing to remove available CAPE, we would expect to see persistently elevated CAPE during the growth of the storm, as reported by Williamson (2013) for CAM4. However, CAPE is fairly low in ALL10, especially between 0400 and 0900, the period when the vertical velocity decreases the most. Additionally, we have conducted as experiment where we halved the value of the deep convection relaxation timescale in the ALL10PA run (from 3600 s to 1800 s), and this has a negligible effect on ω_{500} and precipitation in our case study. This change also increased global mean extreme precipitation to 0.19 mm/d (as opposed to 0.16 mm/d for ALL10PA as seen in Table 6), which is the opposite of the effect we would expect based on results from CAM4 (Williamson, 2013). Taken together, these findings suggest that any increase in grid-point storms at short time steps is not purely the result of weakened deep convection.

4.4 The Role of CLUBB+MG2 Coupling

We close by noting that there are several effects related to the CLUBB+MG2 coupling where further study is needed. For example, the ice water content and high cloud fraction increase significantly when substepping MG2 by itself, but decreases when adjusting the CLUBB+MG2 coupling time step (Table 4). The increase in ice mass from MG2 substepping likely comes from improved resolution of in microphysical process rates, particularly those involving the transfer of mass between ice and vapor phases (Santos et al., 2020). When the CLUBB+MG2 coupling time step is also reduced, the ice cloud fraction is recalculated more frequently. The ice cloud fraction is diagnosed by CLUBB from an effective relative humidity (using total water in the grid box rather than just water vapor). If MG2 causes ice particles to grow and sediment out of the box, this reduces the relative humidity, causing CLUBB to diagnose a smaller cloud fraction. This would explain why substepping CLUBB+MG2 reduces the high cloud fraction. However, confirming this hypothesis, as well as understanding how the reduced cloud fraction interacts with the ice microphysics, would require diagnostics that provide more detailed information about the process rates for CLUBB+MG2 when using different time steps.

We also noticed that substepping CLUBB+MG2 together seems to result in different spatial patterns of precipitation from CTRL, and similar to those seen in the ALL10 case. For instance, compare low-latitude land precipitation across the different simulations in Table 4. As shown in Figure 14a), grid-point storms over land can be stimulated by adjusting the CLUBB+MG2 time step alone, though these storms are much weaker than those that occur in the ALL10 run, and this may account for these changes in precipitation. This seems to imply that more frequent coupling with MG2 causes an increase in condensation, but the mechanism by which this happens is still unclear.

Truly understanding these phenomena will require a more focused study on behavior of the CLUBB+MG2 system at small time steps. This might be easier to study by using CLUBB in a simpler model than EAM, or a single-column case study in EAM, rather than global results. In particular, we hope that this time step sensitivity could be reproduced by coupling CLUBB to a much simpler microphysics scheme than MG2, which would help to narrow down potential causes.

5 Conclusions

EAMv1 at its default 1800 second time step produces very different results from the same model at a 10 second time step, indicating that the release implementation should not be viewed as calculating the "time-resolved" solution to the system of equations that defines the model physics. The amount and regional distribution of precipitation, and especially the radiatively-important partitioning between large-scale and convective precipitation, shows particularly strong sensitivity to the time step size. The cloud radiative forcings also differ by several watts per square meter, indicating that a reduction in the time step would require, at a minimum, significant retuning of the model to produce reasonable results. By experimenting with substepping of model components, we have been able to distinguish three main model time steps that account for most of the changes seen between the 1800s and 10s versions of the model.

First, a reduction of the combined CLUBB and MG2 time step causes the following changes (mostly seen in Table 4):

1. An increase in total precipitation (Figure 8), leading to a reduction in humidity and a reduction in cloud liquid mass below 750 mb (Figures 9 and 10).
2. A reduction in the ratio of convective to large-scale precipitation (Figure 8).
3. Regional changes in precipitation, most notably including a large increase in average precipitation on the maritime continent and in South America, and an increase in extreme precipitation events.
4. A reduction in cloud fraction above 700 mb (Figure 11), causing a large reduction in the magnitudes of both shortwave and longwave radiative cloud forcing (Figure 12).

A much smaller increase in large-scale precipitation can be produced by changing the time step for MG2 alone, and may be caused by a decrease in the rain evaporation rate at short time steps. Otherwise these effects are only seen when CLUBB and MG2 are substepped together, and the ultimate mechanism behind these changes is unclear. We do note that reducing this time step seems to stimulate more condensation from CLUBB in some circumstances, and this may result in more intense grid-scale storms forming over land, driving the changes in precipitation patterns.

Second, a reduction of the dynamics-physics coupling time step (a.k.a. dtime) causes the following changes (mostly seen in Tables 3 and 4):

1. An increase in cloud mass in the upper troposphere, especially in the midlatitudes (Figure 9).
2. An intensification of the changes in precipitation caused by changing the CLUBB+MG2 time step, including an even larger increase in precipitation over tropical land (Figure 2) and extreme precipitation (3).
3. A substantial decrease in cloud fraction below 700 mb, causing further large decreases in radiative cloud forcing, especially for shortwave radiation (Figure 6).

The first of these changes is typical for time discretization error in a sequential-split system. We output diagnostics related to liquid water content after the MG2 scheme runs, i.e. right after it has removed much of the water condensed earlier in the time step. At smaller time steps, this output more accurately reflects the amount of cloud water present when processes are more tightly coupled and the model state varies less between different parts time step.

The other changes related to dynamics-physics coupling seem to reflect a shift towards more convective clouds, despite the fact that the parameterized deep convection is less active. Wan, Zhang, Yan, et al. (2020) has suggested that this is due to changes in coupling between CLUBB and the radiation scheme, since applying radiative cooling more uniformly over CLUBB substeps results in more convective clouds. We have also noticed an increase in the intensity of grid-point storms when the dynamics-physics coupling time step is reduced. We argue that this is because using a shorter time step leads to strengthened *resolved* convection, which in turn prevents the parameterized deep convection from triggering and reduces non-convective cloud cover.

Third, a reduction of the ZM time step causes the following changes (mostly seen in Table 6):

1. A further reduction in cloud liquid mass below 750 mb (Figure 13), though this corresponds to a reduction in net condensation minus evaporation, not an increase in precipitation.
2. A small decrease in cloud fraction everywhere, causing further small decreases in radiative forcings.
3. A further reduction in the ratio of convective to large-scale precipitation. (However, this only occurs when ZM is coupled more frequently with CLUBB and MG2, which in the original code can only be done by reducing dtime.)

These observations indicate that most time step sensitivity in EAMv1 arises from the coupling frequency between parameterizations, which can have a significant influence on climate even when most of the individual parameterizations seem to be well resolved in time. This may be an underappreciated issue, since developers of new parameterizations tend to focus on the time step of their own particular parameterization rather than the frequency with which it is coupled to other parts of a model.

Given this situation, what can be done to reduce the effect of time integration error on model results? In EAMv1, most calculations in the dynamics and many physics parameterizations are already running at a five minute time step or less, even for lower resolution runs. Donahue and Caldwell (2020) found that for a 1° simulation, halving the dynamics-physics coupling frequency only increased model cost by 20%. Our ALL300 run had one-sixth the dtime of the CTRL run, but only required 66% more core-hours per simulated year. Thus our first suggestion is to simply use a smaller dynamics-physics coupling time step.

However, past a certain point, reducing the dynamics-coupling time step will lead to an increase in resolved-scale convection due to tighter coupling between large-scale condensation and the dynamics. This may be difficult or impossible to suppress with the current deep convection parameterization strategy, and will be more severe at higher resolutions. It may be possible to address this by running the deep convection at multiple stages during a given time step, in order to allow the deep convection to process instability that would otherwise be released as large-scale vertical motion by the dynamics.

Alternatively, it may be possible to make further changes to the dynamics-physics coupling to simulate more frequent interaction without requiring direct dynamics-physics interaction. In Wan, Zhang, Rasch, et al. (2020), time step sensitivity in EAMv1 is studied using similar methods to this work. As mentioned previously, that study includes an experiment ("v1_Dribble") where a dribbling method is used to couple all other processes (including the dynamics) to the CLUBB and MG2 loop. In some regions the effect of using the dribbling method is similar to the effect of decreasing the dynamics-physics coupling time step.

The sensitivity of EAMv1 to the CLUBB+MG2 coupling time step is more difficult to address. CLUBB and MG2 together account for a large share of the model cost, so reducing their time steps by a factor of 30 could be around an order of magnitude slower than the default configuration. Since most modelers will not be able to accept such a large increase in computational cost, we can suggest a few other ways of working around this cost in future model development:

1. Reduce the cost of simulating the most expensive physical processes, e.g. by switching to simpler implementations of these processes, or using machine learning to produce cheap approximations to these parameterizations. A parameterization that uses a less accurate approximation for some process, but is able to run at a higher temporal or spatial resolution, may end up being more accurate than a parameterization that uses a more accurate set of equations.
2. Use alternative time integration schemes (e.g. changing the operator splitting method, using higher-order methods) to lower the time integration error at moderate time step sizes.
3. Redesign the physics to separate out processes that have a shorter or longer time scale. In the case of EAMv1, this would mean refactoring CLUBB and MG2 (or any future set of schemes that cause similar issues), in order to isolate the parts of those parameterizations that are most responsible for the time step sensitivity of the overall model. If this subset of physical processes can be calculated much more cheaply than the total cost of CLUBB and MG2, it could then be handled with a more accurate time integration scheme without incurring an excessive cost.

The appropriate strategy to use in this particular case depends on why EAM is so sensitive to the CLUBB+MG2 coupling time step, which is still under investigation. However, it is likely that future versions of EAM would benefit from separating the microphysical processes into "fast" and "slow" subsystems with different characteristic timescales, which would also allow the fast processes to be solved together with CLUBB if necessary.

In practice, errors coming from a coarse temporal resolution are often handled by simply tuning AGCMs so that they match observations when run with longer time step sizes, just as models are tuned for a particular horizontal and vertical resolution. While this is an effective approach for many studies to match current climate observations, if a model relies heavily on tuning to cancel large numerical errors, it is unlikely to have the correct sensitivity to forcing changes. This is especially a concern for studies that use a model to simulate conditions very different from those originally used to tune that model (e.g. for paleoclimate).

We recommend that AGCM developers continue to study time step sensitivity by running experiments with full model physics. Even when the effect of time step on each individual parameterization is well known, the effect of process coupling can affect model behavior in unpredictable ways. Most users cannot afford to use sub-minute time steps for the entire model, and therefore are likely using a model that is not achieving its own converged small-time-step behavior. Therefore it is important to understand the limitations and biases present in workhorse models that have been tuned for coarse time step sizes.

Acknowledgments

We would like to thank two anonymous reviewers for this paper, whose contributions undoubtedly helped us to paint a clearer and more complete picture.

The data used in this paper is available at:

`https://dabdceba-6d04-11e5-ba46-22000b92c6ec.e.globus.org/publications/Santos_JAMES_2020.tar.gz`

This tar file contains the data used to produce all tables and plots in this paper, and a README explaining the files provided.

The code used to process the data in this study is available at:

`https://github.com/quantheory/E3SMTimestepStudy/tree/james-2020`

or:

`https://doi.org/10.5281/zenodo.4560808`

In addition to the scripts used for data analysis, this repository also contains the file zm_diff.patch, which contains the E3SM modifications used to implement ZM substepping in the ZM10PA and CLUBBMICRO10ZM10PA runs, and the file cld_diff.patch, which contains the implementation for the joint ZM+CLUBB+MG2 substepping in the CLD10PA run.

This research was funded by the U.S. Department of Energy, Office of Science, Office of Biological and Environmental Research. Sean Patrick Santos was further supported during this research by the Seattle chapter of the ARCS Foundation, which provided a scholarship to support his doctoral studies.

References

Balaji, V., Benson, R., Wyman, B., & Held, I. (2016). Coarse-grained component concurrency in earth system modeling: parallelizing atmospheric radiative transfer in the GFDL AM3 model using the Flexible Modeling System coupling framework. *Geoscientific Model Development*, *9*(10), 3605–3616. Retrieved from `https://gmd.copernicus.org/articles/9/3605/2016/` doi: 10.5194/gmd-9-3605-2016

Beljaars, A., Balsamo, G., Bechtold, P., Bozzo, A., Forbes, R., Hogan, R. J., ... Wedi, N. (2018). The numerics of physical parametrization in the ECMWF model. *Frontiers in Earth Science*, *6*, 137. Retrieved from `https://www.frontiersin.org/article/10.3389/feart.2018.00137` doi: 10.3389/feart.2018.00137

Beljaars, A., Bechtold, P., Köhler, M., Morcrette, J.-J., Tompkins, A., Viterbo, P., & Wedi, N. (2004). The numerics of physical parameterization. In *Seminar on recent developments in numerical methods for atmospheric and ocean modelling, 6-10 september 2004* (p. 113-134). Shinfield Park, Reading: ECMWF. Retrieved from `https://www.ecmwf.int/node/8032`

Chosson, F., Vaillancourt, P. A., Milbrandt, J. A., Yau, M. K., & Zadra, A. (2014). Adapting two-moment microphysics schemes across model resolutions: Subgrid cloud and precipitation fraction and microphysical sub–time step. *Journal of the Atmospheric Sciences*, *71*(7), 2635-2653. Retrieved from `https://doi.org/10.1175/JAS-D-13-0367.1` doi: 10.1175/JAS-D-13-0367.1

Diamantakis, M., Davies, T., & Wood, N. (2007). An iterative time-stepping scheme for the Met Office's semi-implicit semi-Lagrangian non-hydrostatic model. *Quarterly Journal of the Royal Meteorological Society*, *133*(625), 997-1011. Retrieved from https://rmets.onlinelibrary.wiley.com/doi/abs/10.1002/qj.59 doi: https://doi.org/10.1002/qj.59

Donahue, A. S., & Caldwell, P. M. (2018). Impact of physics parameterization ordering in a global atmosphere model. *Journal of Advances in Modeling Earth Systems*, *10*(2), 481-499. Retrieved from https://agupubs.onlinelibrary.wiley.com/doi/abs/10.1002/2017MS001067 doi: 10.1002/2017MS001067

Donahue, A. S., & Caldwell, P. M. (2020). Performance and accuracy implications of parallel split physics-dynamics coupling in the Energy Exascale Earth System Atmosphere Model. *Journal of Advances in Modeling Earth Systems*, *12*(7), e2020MS002080. Retrieved from https://agupubs.onlinelibrary.wiley.com/doi/abs/10.1029/2020MS002080 (e2020MS002080 10.1029/2020MS002080) doi: 10.1029/2020MS002080

Dubal, M., Wood, N., & Staniforth, A. (2005). Mixed parallel–sequential-split schemes for time-stepping multiple physical parameterizations. *Monthly Weather Review*, *133*(4), 989-1002. Retrieved from https://doi.org/10.1175/MWR2893.1 doi: 10.1175/MWR2893.1

Gettelman, A., & Morrison, H. (2015). Advanced two-moment bulk microphysics for global models. part I: Off-line tests and comparison with other schemes. *Journal of Climate*, *28*(3), 1268-1287. Retrieved from https://doi.org/10.1175/JCLI-D-14-00102.1 doi: 10.1175/JCLI-D-14-00102.1

Gettelman, A., Morrison, H., Santos, S., Bogenschutz, P., & Caldwell, P. (2015). Advanced two-moment bulk microphysics for global models. part II: Global model solutions and aerosol–cloud interactions. *Journal of Climate*, *28*(3), 1288–1307. Retrieved from http://journals.ametsoc.org/doi/full/10.1175/JCLI-D-14-00103.1 doi: 10.1175/JCLI-D-14-00103.1

Golaz, J.-C., Caldwell, P. M., Van Roekel, L. P., Petersen, M. R., Tang, Q., Wolfe, J. D., … Zhu, Q. (2019). The DOE E3SM coupled model version 1: Overview and evaluation at standard resolution. *Journal of Advances in Modeling Earth Systems*, *11*(7), 2089-2129. Retrieved from https://agupubs.onlinelibrary.wiley.com/doi/abs/10.1029/2018MS001603 doi: 10.1029/2018MS001603

Gross, M., Wan, H., Rasch, P. J., Caldwell, P. M., Williamson, D. L., Klocke, D., … Leung, R. (2018). Physics-dynamics coupling in weather, climate, and earth system models: Challenges and recent progress. *Monthly Weather Review*, *146*(11), 3505 - 3544. Retrieved from https://journals.ametsoc.org/view/journals/mwre/146/11/mwr-d-17-0345.1.xml doi: 10.1175/MWR-D-17-0345.1

Herrington, A. R., & Reed, K. A. (2017). An explanation for the sensitivity of the mean state of the Community Atmosphere Model to horizontal resolution on aquaplanets. *Journal of Climate*, *30*(13), 4781 - 4797. Retrieved from https://journals.ametsoc.org/view/journals/clim/30/13/jcli-d-16-0069.1.xml doi: 10.1175/JCLI-D-16-0069.1

Herrington, A. R., & Reed, K. A. (2018). An idealized test of the response of the Community Atmosphere Model to near-grid-scale forcing across hydrostatic resolutions. *Journal of Advances in Modeling Earth Systems*, *10*(2), 560-575. Retrieved from https://agupubs.onlinelibrary.wiley.com/doi/abs/10.1002/2017MS001078 doi: https://doi.org/10.1002/2017MS001078

Lebassi-Habtezion, B., & Caldwell, P. M. (2015). Aerosol specification in single-column Community Atmosphere Model version 5. *Geoscientific Model Development*, *8*(3), 817–828. Retrieved from https://gmd.copernicus.org/articles/8/817/2015/ doi: 10.5194/gmd-8-817-2015

Mishra, S. K., & Shanay, S. (2011). Effects of time step size on the simulation of tropical climate in NCAR-CAM3. *Climate Dynamics*, *37*(3), 689-704. Retrieved from https://doi.org/10.1007/s00382-011-0994-4 doi: 10.1007/s00382-011-0994-4

Mishra, S. K., Srinivasan, J., & Nanjundiah, R. S. (2008). The impact of the time step on the intensity of ITCZ in an aquaplanet GCM. *Monthly Weather Review*, *136*(11), 4077-4091. Retrieved from https://doi.org/10.1175/2008MWR2478.1 doi: 10.1175/2008MWR2478.1

Posselt, R., & Lohmann, U. (2008). Introduction of prognostic rain in ECHAM5: design and single column model simulations. *Atmospheric Chemistry and Physics*, *8*(11), 2949–2963. Retrieved from https://www.atmos-chem-phys.net/8/2949/2008/ doi: 10.5194/acp-8-2949-2008

Rasch, P. J., Xie, S., Ma, P.-L., Lin, W., Wang, H., Tang, Q., ... Yang, Y. (2019). An overview of the atmospheric component of the Energy Exascale Earth System Model. *Journal of Advances in Modeling Earth Systems*, *11*(8), 2377-2411. Retrieved from https://agupubs.onlinelibrary.wiley.com/doi/abs/10.1029/2019MS001629 doi: 10.1029/2019MS001629

Riette, S. (2020). Development of “Physical Parametrizations with PYthon” (PPPY, version 1.1) and its usage to reduce the time-step dependency in a microphysical scheme. *Geoscientific Model Development*, *13*(2), 443–460. Retrieved from https://gmd.copernicus.org/articles/13/443/2020/ doi: 10.5194/gmd-13-443-2020

Santos, S. P., Caldwell, P. M., & Bretherton, C. S. (2020). Numerically relevant timescales in the MG2 microphysics model. *Journal of Advances in Modeling Earth Systems*, *12*(4), e2019MS001972. Retrieved from https://agupubs.onlinelibrary.wiley.com/doi/abs/10.1029/2019MS001972 (e2019MS001972 10.1029/2019MS001972) doi: 10.1029/2019MS001972

Strang, G. (1968). On the construction and comparison of difference schemes. *SIAM Journal on Numerical Analysis*, *5*(3), 506-517. Retrieved from https://doi.org/10.1137/0705041 doi: 10.1137/0705041

Walters, D., Baran, A. J., Boutle, I., Brooks, M., Earnshaw, P., Edwards, J., ... Zerroukat, M. (2019). The Met Office Unified Model Global Atmosphere 7.0/7.1 and JULES Global Land 7.0 configurations. *Geoscientific Model Development*, *12*(5), 1909–1963. Retrieved from https://gmd.copernicus.org/articles/12/1909/2019/ doi: 10.5194/gmd-12-1909-2019

Wan, H., Rasch, P. J., Taylor, M. A., & Jablonowski, C. (2015). Short-term time step convergence in a climate model. *Journal of Advances in Modeling Earth Systems*, *7*(1), 215-225. Retrieved from https://agupubs.onlinelibrary.wiley.com/doi/abs/10.1002/2014MS000368 doi: 10.1002/2014MS000368

Wan, H., Rasch, P. J., Zhang, K., Kazil, J., & Leung, L. R. (2013). Numerical issues associated with compensating and competing processes in climate models: an example from ECHAM-HAM. *Geoscientific Model Development*, *6*(3), 861–874. Retrieved from https://gmd.copernicus.org/articles/6/861/2013/ doi: 10.5194/gmd-6-861-2013

Wan, H., Rasch, P. J., Zhang, K., Qian, Y., Yan, H., & Zhao, C. (2014). Short ensembles: an efficient method for discerning climate-relevant sensitivities in atmospheric general circulation models. *Geoscientific Model Development*, *7*(5), 1961–1977. Retrieved from https://www.geosci-model-dev.net/7/1961/2014/ doi: 10.5194/gmd-7-1961-2014

Wan, H., Zhang, S., Rasch, P. J., Larson, V. E., Zeng, X., & Yan, H. (2020). Quantifying and attributing time step sensitivities in present-day climate simulations conducted with EAMv1. *Geoscientific Model Development Discussions*, *2020*, 1–36. Retrieved from https://gmd.copernicus.org/preprints/gmd-2020-330/ doi: 10.5194/gmd-2020-330

Wan, H., Zhang, S., Yan, H., Larson, V., Zhang, K., Singh, B., & Rasch, P. (2020). *Numerical coupling of atmospheric processes and its impact on subtropical marine clouds in EAMv1.* Retrieved from https://www.cesm.ucar.edu/events/wg-meetings/2020/files/atmos/Wan.pdf (Lecture delivered at 2020 Joint Winter Meeting of CESM Atmosphere Model, Whole Atmosphere and

Chemistry-Climate Working Groups.)

Williamson, D. L. (2008). Convergence of aqua-planet simulations with increasing resolution in the Community Atmospheric Model, version 3. *Tellus A*, *60*(5), 848-862. Retrieved from https://onlinelibrary.wiley.com/doi/abs/10.1111/j.1600-0870.2008.00339.x doi: 10.1111/j.1600-0870.2008.00339.x

Williamson, D. L. (2013). The effect of time steps and time-scales on parametrization suites. *Quarterly Journal of the Royal Meteorological Society*, *139*(671), 548-560. Retrieved from https://rmets.onlinelibrary.wiley.com/doi/abs/10.1002/qj.1992 doi: 10.1002/qj.1992

Williamson, D. L., & Olson, J. G. (2003). Dependence of aqua-planet simulations on time step. *Quarterly Journal of the Royal Meteorological Society*, *129*(591), 2049-2064. Retrieved from https://rmets.onlinelibrary.wiley.com/doi/abs/10.1256/qj.02.62 doi: 10.1256/qj.02.62

Xie, S., Lin, W., Rasch, P. J., Ma, P.-L., Neale, R., Larson, V. E., ... Zhang, Y. (2018). Understanding cloud and convective characteristics in version 1 of the E3SM Atmosphere Model. *Journal of Advances in Modeling Earth Systems*, *10*(10), 2618-2644. Retrieved from https://agupubs.onlinelibrary.wiley.com/doi/abs/10.1029/2018MS001350 doi: 10.1029/2018MS001350

Yu, S., & Pritchard, M. S. (2015). The effect of large-scale model time step and multiscale coupling frequency on cloud climatology, vertical structure, and rainfall extremes in a superparameterized GCM. *Journal of Advances in Modeling Earth Systems*, *7*(4), 1977-1996. Retrieved from https://agupubs.onlinelibrary.wiley.com/doi/abs/10.1002/2015MS000493 doi: 10.1002/2015MS000493

Zheng, X., Klein, S. A., Ghate, V. P., Santos, S., McGibbon, J., Caldwell, P., ... Cadeddu, M. P. (2020, 07). Assessment of Precipitating Marine Stratocumulus Clouds in the E3SMv1 Atmosphere Model: A Case Study from the ARM MAGIC Field Campaign. *Monthly Weather Review*, *148*(8), 3341-3359. Retrieved from https://doi.org/10.1175/MWR-D-19-0349.1 doi: 10.1175/MWR-D-19-0349.1